

Matrix models, gauge theory and emergent geometry

This article has been downloaded from IOPscience. Please scroll down to see the full text article.

JHEP05(2009)049

(<http://iopscience.iop.org/1126-6708/2009/05/049>)

[The Table of Contents](#) and [more related content](#) is available

Download details:

IP Address: 80.92.225.132

The article was downloaded on 03/04/2010 at 09:19

Please note that [terms and conditions apply](#).

Matrix models, gauge theory and emergent geometry

Rodrigo Delgadillo-Blando,^{a,b} Denjoe O'Connor^a and Badis Ydri^c

^a*School of Theoretical Physics, DIAS,
10 Burlington Road, Dublin 4, Ireland*

^b*Departamento de Física, CINVESTAV-IPN,
Apdo. 14-740, 07000, México, D.F. México*

^c*Institut für Physik, Humboldt-Universität zu Berlin,
D-12489 Berlin, Germany*

E-mail: rodrigo@stp.dias.ie, denjoe@stp.dias.ie, ydri@stp.dias.ie

ABSTRACT: We present, theoretical predictions and Monte Carlo simulations, for a simple three matrix model that exhibits an exotic phase transition. The nature of the transition is very different if approached from the high or low temperature side. The high temperature phase is described by three self interacting random matrices with no background spacetime geometry. As the system cools there is a phase transition in which a classical two-sphere condenses to form the background geometry. The transition has an entropy jump or latent heat, yet the specific heat diverges as the transition is approached from low temperatures. We find no divergence or evidence of critical fluctuations when the transition is approached from the high temperature phase. At sufficiently low temperatures the system is described by small fluctuations, on a background classical two-sphere, of a U(1) gauge field coupled to a massive scalar field. The critical temperature is pushed upwards as the scalar field mass is increased. Once the geometrical phase is well established the specific heat takes the value 1 with the gauge and scalar fields each contributing 1/2.

KEYWORDS: Matrix Models, Non-Commutative Geometry, Gauge Symmetry, Nonperturbative Effects

ARXIV EPRINT: [0806.0558](https://arxiv.org/abs/0806.0558)

The author B.Y. dedicates this work to the memory of his daughter Nour (24-Nov 06,28-Jun 07)

Contents

1	Introduction	1
2	The fuzzy sphere	3
3	Theoretical predictions	4
3.1	Gauge action	4
3.2	Matrix model	5
3.3	Quantization and observables for small m^2	7
3.4	Phase transitions	9
3.5	Predictions from the effective potential	12
3.6	Critical behaviour	14
3.7	The generic case	15
4	Numerical results	18
4.1	The theory with $m^2 = 0$	18
4.2	The action, radius and specific heat for $m^2 \neq 0$	20
4.3	The limit $m^2 \rightarrow \infty$ and specific heat	21
4.4	The phase diagram	24
4.5	The eigenvalue distributions for large m^2	26
4.5.1	The low temperature phase (fuzzy sphere)	26
4.5.2	The high temperature phase (matrix phase)	28
4.6	Emergent geometry	29
4.7	The model with only pure potential term	30
4.8	The Chern-Simons+potential model	31
5	Conclusion and outlook	34

1 Introduction

All the fundamental laws of physics are now understood in geometrical terms. The classical geometry that plays a fundamental role in our formulation of these laws has been vastly extended in noncommutative geometry [1]. However, we still have very little insight into the origins of spacetime geometry itself. This situation has been undergoing a significant evolution in recent years and it now seems possible to understand geometry as an emergent concept. The notion of geometry as an emergent concept is not new, see for example [2] for an inspiring discussion and [3, 4] for some recent ideas. We examine such a phenomenon in the context of a simple three matrix model [5–7].

Matrix models with a background noncommutative geometry have received attention as an alternative setting for the regularization of field theories [8–11] and as the configurations of $D0$ branes in string theory [12, 13]. In the model studied here, the situation is quite different. It has no background geometry in the high temperature phase and the geometry itself emerges as the system cools, much as a Bose condensate or superfluid emerges as a collective phenomenon at low temperatures. The simplicity of the model we study here allows for a detailed examination of such an exotic transition. We suspect the characteristic features of the transition may be generic to this novel phenomenon.

In this article we study both theoretically and numerically a three matrix model with global $SO(3)$ symmetry whose energy functional or Euclidean action functional (see eq. (3.6)) is a single trace of a quartic polynomial in the matrices D_a . The model contains three parameters, the inverse temperature $\beta = \tilde{\alpha}^4 = g^{-2}$, and parameters m and μ which provide coefficients for the quartic and quadratic terms in the potential.

We find that as the parameters are varied the model has a phase transition with two clearly distinct phases, one *geometrical* the other a *matrix phase*. Small fluctuations in the *geometrical phase* are those of a Yang-Mills and a scalar field around a ground state corresponding to a round two-sphere. In the *matrix phase* there is no background spacetime geometry and the fluctuations are those of the matrix entries around zero. In this article we focus on the subset of parameter space where in the large matrix limit the gauge group is Abelian.

For finite but large N , at low temperature, the model exhibits fluctuations around a fuzzy sphere [14]. In the infinite N limit the macroscopic geometry becomes classical. As the temperature is increased it undergoes a transition with latent heat so the entropy jumps, yet the model has critical fluctuations and a divergent specific heat. As this critical coupling is approached the fuzzy sphere radius expands to a critical radius and the sphere evaporates. The neighbourhood of the critical point exhibits all the standard symptoms of a continuous 2nd order transition, such as large scale fluctuations, critical slowing down (of the Monte Carlo routine) and is characterized by a specific heat exponent which we argue is $\alpha = 1/2$, a value consistent with our numerical simulations. In the high temperature (strong coupling) phase the model is a matrix model closely related to zero dimensional Yang-Mills theory. As the transition is approached from within this phase we find no evidence of critical fluctuations and no divergence in the specific heat.

In the *geometrical sphere* phase the gauge coupling constant is $g^2 = \beta^{-1}$ and m parameterizes the mass of the scalar field. For small m^2 we find a transition with discontinuous internal energy $U = \langle S \rangle / \beta$ (so the entropy jumps across the transition [15]) while the specific heat is divergent as the transition is approached from the low temperature fuzzy sphere phase but finite when approached from the high temperature *matrix phase*. The fuzzy sphere emerges as the low temperature ground state which as one expects is the low entropy phase and the transition is characterized by both a latent heat and divergent fluctuations.

To our knowledge it is the first clear example of a transition where the spacetime geometry is emergent. This transition itself is extremely unusual. We know of no other physical situation that has a transition with these features. Standard transitions are very dependent on the dimension of the background spacetime and when this is itself in transition an asymmetry of the approach to criticality is not so surprising.

By studying the eigenvalues of operators in the theory we establish that, in the matrix phase, the matrices D_a are characterised by continuous eigenvalue distributions which undergo a transition to a point spectrum characteristic of the fuzzy sphere phase as the temperature is lowered. The point spectrum is consistent with $D_a = L_a/R$ where L_a are $su(2)$ angular momentum generators in the irreducible representation given by the matrix size and R is the radius of the fuzzy sphere. The full model received an initial study in [7] while a simpler version, invariant under translations of D_a , arises naturally as the configuration of $D0$ branes in the large k limit of a boundary Wess-Zumino-Novikov-Witten model [13] and has been studied numerically in [5]. If the mass parameters of the potential are related to the matrix size, the model becomes that introduced in [16]. The interpretation presented here is novel, as are the results on the entropy and critical behaviour and the extension to the full model.

A short description of the results obtained in this article is given in [15]. This article is organised as follows. In section 2 we review the fuzzy sphere and its geometry. In section 3 we derive several theoretical predictions in the fuzzy sphere phase including the critical behaviour of the model. In section 4 we discuss the non-perturbative phase structure (phase diagram) and Monte Carlo numerical results for various observables. We conclude in section 5 with some discussion and speculations.

2 The fuzzy sphere

The ordinary round unit sphere, S^2 , can be defined as the two dimensional surface embedded in flat three dimensional space satisfying the equation $\sum_{a=1}^3 n_a^2 = 1$ with $\vec{n} \in R^3$. One can use the n_a as a nonholonomic coordinate system for the sphere. In this coordinate system a general function can be expanded as $f(\vec{n}) = \sum_{l=0}^{\infty} f_{lm} Y_{lm}(\vec{n})$, where Y_{lm} are the standard spherical harmonics. The basic derivations are provided by the $SO(3)$ generators defined by $\mathcal{L}_a = -i\epsilon_{abc} n_b \partial_c$ and the Laplacian is $\mathcal{L}^2 = \mathcal{L}_a \mathcal{L}_a$ with eigenvalues $l(l+1)$, $l = 0, \dots, \infty$. Following Fröhlich and Gawędzki [25] (or Connes [1] for spin geometry) the geometry of a Riemannian manifold can be encoded in a spectral triple. For the ordinary sphere the triple is $(C^\infty(\mathbf{S}^2), \mathcal{H}, \mathcal{L}^2)$ where $C^\infty(S^2)$ is the algebra of all functions $f(\vec{n})$ on the sphere and \mathcal{H} is the infinite dimensional Hilbert space of square integrable functions. Such a spectral triple is precisely the data that enters the scalar field action on the manifold. So a scalar field action which includes an appropriate Laplacian can specify the geometry.

The fuzzy sphere can be viewed as a particular deformation of the above triple which is based on the fact that the sphere is the coadjoint orbit $SU(2)/U(1)$ [14],

$$g\sigma_3g^{-1} = n_a\sigma_a, \quad g \in SU(2), \quad \vec{n} \in S^2, \tag{2.1}$$

and is therefore a symplectic manifold which can be quantized in a canonical fashion by simply quantizing the volume form

$$\omega = \sin\theta d\theta \wedge d\phi = \frac{1}{2}\epsilon_{abc} n_a dn_b \wedge dn_c. \tag{2.2}$$

The result of this quantization is to replace the algebra $C^\infty(S^2)$ by the algebra of $N \times N$ matrices Mat_N . Mat_N becomes the N^2 -dimensional Hilbert space structure H_N when

supplied with inner product $(f, g) = \frac{1}{N} \text{Tr}(f^\dagger g)$ where $f, g \in \text{Mat}_N$. The spin $\frac{N-1}{2}$ IRR of $su(2)$ has both a left and a right action on this Hilbert space. For the left action the generators are L_a and satisfying $[L_a, L_b] = i\epsilon_{abc}L_c$, and $\sum_a L_a^2 = c_2 = \frac{N^2-1}{4}$. The spherical harmonics $Y_{lm}(\vec{n})$ become the canonical $su(2)$ polarization tensors \hat{Y}_{lm} and form a basis for H_N . These are defined by

$$\left[L_a, \left[L_a, \hat{Y}_{lm} \right] \right] = l(l+1)\hat{Y}_{lm}, \quad \left[L_\pm, \hat{Y}_{lm} \right] = \sqrt{(l \mp m)(l \pm m + 1)}\hat{Y}_{lm \pm 1}, \quad \left[L_3, \hat{Y}_{lm} \right] = m\hat{Y}_{lm}. \tag{2.3}$$

and satisfy

$$\hat{Y}_{lm}^\dagger = (-1)^m \hat{Y}_{l, -m}, \quad \frac{1}{N} \text{Tr} \hat{Y}_{l_1 m_1} \hat{Y}_{l_2 m_2} = (-1)^{m_1} \delta_{l_1 l_2} \delta_{m_1, -m_2}, \tag{2.4}$$

and the completeness relation

$$\sum_{l=0}^{N-1} \sum_{m=-l}^l \hat{Y}_{lm}^\dagger \hat{Y}_{lm} = \mathbf{1} \tag{2.5}$$

The ‘‘coordinates functions’’ on the fuzzy sphere S_N^2 are defined to be proportional to $\hat{Y}_{1\mu}$ tensors (as in the continuum) and satisfy

$$x_1^2 + x_2^2 + x_3^2 = 1, \quad [x_a, x_b] = \frac{i}{\sqrt{c_2}} \epsilon_{abc} x_c, \quad \text{where } x_a = \frac{L_a}{\sqrt{c_2}}. \tag{2.6}$$

‘‘Fuzzy’’ functions on S_N^2 are elements of the matrix algebra while derivations are inner and given by the generators of the adjoint action of $su(2)$ defined by $\hat{\mathcal{L}}_a \phi := [L_a, \phi]$. A natural choice of the Laplacian on the fuzzy sphere is therefore given by the Casimir operator

$$\hat{\mathcal{L}}^2 = [L_a, [L_a, \dots]]. \tag{2.7}$$

Thus the algebra of matrices Mat_N with $N = L + 1$ decomposes under the action of $su(2)$ as $\frac{L}{2} \otimes \frac{L}{2} = 0 \oplus 1 \oplus 2 \oplus \dots \oplus L$, with the first $\frac{L}{2}$ standing for the left action while the other $\frac{L}{2}$ stands for the right action of $su(2)$. It is not difficult to convince ourselves that this Laplacian has a cut-off spectrum with eigenvalues $l(l+1)$ where $l = 0, 1, \dots, L$. Given the above discussion we see that a general fuzzy function (or element of the algebra) on S_N^2 can be expanded in terms of polarization tensors as follows $f = \sum_{l=0}^L \sum_{m=-l}^l f_{lm} \hat{Y}_{lm}$. The continuum limit is given by $L \rightarrow \infty$. Therefore the fuzzy sphere can be described as a sequence of triples $(\text{Mat}_N, H_N, \hat{\mathcal{L}}^2)$ with a well defined limit given by the triple $(C^\infty(\mathbf{S}^2), \mathcal{H}, \mathcal{L}^2)$. The number of degrees of freedom in the function algebra of \mathbf{S}_N^2 is N^2 and the noncommutativity parameter is $\theta = \frac{2}{\sqrt{N^2-1}}$.

3 Theoretical predictions

3.1 Gauge action

It has been shown in [26–29] that the differential calculus on the fuzzy sphere is three dimensional and as a consequence, treating gauge fields as one-forms, a generic gauge field,

\vec{A} has 3 components. Each component A_a , $a = 1, 2, 3$, is an element of Mat_N and the $U(1)$ gauge symmetry of the commutative sphere will become a $U(N)$ gauge symmetry on the fuzzy sphere with gauge transformations implemented as $A_a \rightarrow U A_a U^\dagger + U[L_a, U^\dagger]$ where $U \in U(N)$. In this approach to gauge fields on the fuzzy sphere, \mathbf{S}_N^2 , it is difficult to split the vector field \vec{A} in a gauge-covariant fashion into a tangent gauge field and a normal scalar field. However, we can write a gauge-covariant expression for the normal scalar field as $\Phi = \frac{1}{2}(x_a A_a + A_a x_a + \frac{A_a^2}{\sqrt{c_2}})$. In the commutative limit, $N \rightarrow \infty$, we have $A_a \rightarrow \mathcal{A}_a$ and $\Phi \rightarrow \varphi = n_a \mathcal{A}_a$ and the splitting into gauge field and scalar field becomes trivial being implemented by simply writing $\mathcal{A}_a = n_a \varphi + a_a$, with $n_a a_a = 0$, where \vec{n} is the unit vector on \mathbf{S}^2 , $\varphi = \vec{n} \cdot \vec{\mathcal{A}}$ is the normal gauge-invariant component of $\vec{\mathcal{A}}$ and \vec{a} is the tangent gauge field.

For this formulation of gauge field theory on the fuzzy sphere the most general action (up to quartic power in A_a) on \mathbf{S}_N^2 is then

$$S_N[A] = \frac{1}{4g^2 N} Tr F_{ab}^2 - \frac{1}{2g^2 N} \epsilon_{abc} Tr \left[\frac{1}{2} F_{ab} A_c - \frac{i}{6} [A_a, A_b] A_c \right] + \frac{2m^2}{g^2 N} Tr \Phi^2 + \frac{\rho}{g^2 N} Tr \Phi. \tag{3.1}$$

In above $Tr \mathbf{1} = N$ and $F_{ab} = i[L_a, A_b] - i[L_b, A_a] + \epsilon_{abc} A_c + i[A_a, A_b]$ is the covariant curvature, and $S_N[0] = 0$. The limit $m^2 \rightarrow \infty$ gives a large mass to the scalar component and effectively projects it out of the spectrum of small fluctuations.

The associated continuum action S_∞ is then at most quadratic in the field and as a consequence the theory is largely trivial, consisting of a gauge field and a scalar field that have a mixing in their joint propagator. Indeed we can show that

$$S_\infty = \frac{1}{4g^2} \int \frac{d\Omega}{4\pi} \left[(f_{ab})^2 - 4\epsilon_{abc} f_{ab} n_c \varphi - 2(\mathcal{L}_a \varphi)^2 + 4(1 + 2m^2)\varphi^2 + 4\rho\varphi \right], \tag{3.2}$$

where f_{ab} is the curvature of the tangent field a_a and $f_{ab} = i\mathcal{L}_a a_b - i\mathcal{L}_b a_a + \epsilon_{abc} a_c$. As one can immediately see this theory consists of a 2-component gauge field a_a that mixes with a scalar field φ , i.e. the propagator mixes the two fields. In the following we will primarily be interested in the case with $\rho = 0$. We see also that the presence of the scalar field means that the geometry is completely specified, in that all the ingredients of the spectral triple are supplied by this field. In contrast a two dimensional gauge theory on its own would not be sufficient to specify the geometry.

3.2 Matrix model

We introduce $\tilde{\alpha}^4 = \frac{1}{g^2} = \beta$ where β can be interpreted as an inverse temperature and we can rewrite the above gauge action (3.1) (shifted by constants and dropping the subscript

N) in terms of $D_a = L_a + A_a$ as follows:

$$\begin{aligned}
 S^{(0)}[D] &= \frac{1}{4g^2N} \text{Tr} F_{ab}^2 - \frac{1}{2g^2N} \epsilon_{abc} \text{Tr} \left[\frac{1}{2} F_{ab} A_c - \frac{i}{6} [A_a, A_b] A_c \right] - \frac{\tilde{\alpha}^4 c_2}{6} \\
 &= \frac{\tilde{\alpha}^4}{N} \left[-\frac{1}{4} \text{Tr} [D_a, D_b]^2 + \frac{2i}{3} \epsilon_{abc} \text{Tr} D_a D_b D_c \right].
 \end{aligned} \tag{3.3}$$

$$\begin{aligned}
 V[D] &= \frac{2m^2}{g^2N} \text{Tr} \Phi^2 + \frac{\rho}{g^2N} \text{Tr} \Phi - \frac{m^2 c_2}{2g^2} + \frac{\rho \sqrt{c_2}}{2g^2} \\
 &= \frac{\tilde{\alpha}^4}{N} \left[\frac{m^2}{2c_2} \text{Tr} (D_a^2)^2 + \left(\frac{\rho}{2\sqrt{c_2}} - m^2 \right) \text{Tr} (D_a^2) \right].
 \end{aligned} \tag{3.4}$$

The complete action functional is then:

$$S[D] \equiv S^{(0)}[D] + V[D] = S_N[A] - \frac{\tilde{\alpha}^4 c_2}{6} - \frac{\tilde{\alpha}^4 m^2 c_2}{2} + \frac{\tilde{\alpha}^4 \rho \sqrt{c_2}}{2}, \tag{3.5}$$

and the constants are chosen so that $S[0] = 0$. The action takes the rather simple form

$$S[D] = \frac{\tilde{\alpha}^4}{N} \text{Tr} \left[-\frac{1}{4} [D_a, D_b]^2 + \frac{2i}{3} \epsilon_{abc} D_a D_b D_c + \frac{m^2}{2c_2} (D_a^2)^2 - \mu D_a^2 \right] \tag{3.6}$$

where $\mu = m^2 - \frac{\rho}{2\sqrt{c_2}}$. It is invariant under unitary transformations $U(N)$ and global rotations $SO(3)$. Extrema of the model are given by the reducible representations of $SU(2)$ and commuting matrices. For sufficiently small ρ and with $c_2 = (N^2 - 1)/4$ the classical absolute minima of the model is given by the irreducible representation of $SU(2)$ of dimension N . Small fluctuations around this background can then be seen to have the geometrical content of a Yang-Mills and scalar multiplet on a background fuzzy sphere as described in the previous section. As we will see, for small enough coupling or low temperature, these configurations also give the ground state of the fluctuating system. For very small negative values of the parameter μ , and for $m = 0$ there is a local minimum at $D_a = 0$ and a global minimum at $D_a \sim L_a$, separated by a barrier. As μ is made more negative the difference in energy (or Euclidean action) between the two extrema becomes less and eventually for $\mu = -\frac{2}{9}$ the two minima become degenerate, one occurring at $D_a = 0$ while the other occurs at $D_a = \frac{2}{3}L_a$ and they are separated by a barrier whose maximum occurs at $D_a = \frac{1}{3}L_a$.

In this special case (i.e. $m = 0$ and $\mu = -\frac{2}{9}$ or equivalently $\rho = \frac{4}{9}\sqrt{c_2}$) the action takes the form

$$S[D] = \frac{\tilde{\alpha}^4}{N} \left(\frac{i}{2} \text{Tr} [D_a, D_b] + \frac{1}{3} \epsilon_{abc} D_c \right)^2. \tag{3.7}$$

and we see that the configurations $D_a = 0$ and $D_a = \frac{2}{3}L_a$ both give zero action, however there is a unique configuration with $D_a = 0$ while there is an entire $SU(N)$ manifold of configurations $D_a = \frac{2}{3}UL_aU^\dagger$ which are equivalent. The classical model has a first order transition at $m = 0$ for $\mu = -\frac{2}{9}$ and the classical ground state switches from $D_a = \phi L_a$, where $\phi = (1 + \sqrt{1 + 4\mu})/2$, for $\mu > -2/9$ to $D_a = 0$ for $\mu < -2/9$. The quantity ϕ is therefore a useful order parameter for this transition. However, one would expect fluctuations to have a significant effect on this classical picture.

In fact both theoretical and numerical studies show that in the fluctuating theory, the fuzzy sphere phase only exists for $\mu > -2/9$ [30].

3.3 Quantization and observables for small m^2

The quantum version of the model is taken to be that obtained by functional integration with respect to the gauge field. This amounts to integration over the three Hermitian matrices D_a with Dyson measure and the partition function Z is given by

$$Z = \int dD_a e^{-S[D]} = e^{-\frac{3N^2}{4} \log \alpha^4} \int dX_a e^{-N\hat{S}[X]}, \quad X_a = \alpha D_a, \quad \tilde{\alpha} = \alpha\sqrt{N}$$

$$\hat{S}[X] = -\frac{1}{4} \text{Tr}[X_a, X_b]^2 + \frac{2i\alpha}{3} \epsilon_{abc} \text{Tr} X_a X_b X_c + \frac{m^2}{2c_2} \text{Tr}(X_a^2)^2 + \left(\frac{\rho\alpha^2}{2\sqrt{c_2}} - m^2\alpha^2 \right) \text{Tr}(X_a^2). \quad (3.8)$$

The latter form of the expression (in terms of X_a) allows us to take $\tilde{\alpha} = 0$ and we see that this limit is equivalent to removing all but the leading commutator squared term. Also the quartic term proportional to m^2 survives. However if m^2 and ρ are scaled appropriately with $\tilde{\alpha}$ only the Chern-Simons term $\epsilon_{abc} \text{Tr} X_a X_b X_c$ is removed.

The set of gauge equivalent configurations is parameterized by the $SU(N)$ group manifold which is compact, so there is no need to gauge fix and the functional integral is well defined, being an ordinary integral over \mathbf{R}^{3N^2} . However, the volume of the gauge group diverges in the limit $N \rightarrow \infty$ and to make contact with the commutative formulation it is convenient to gauge fix in the standard way.

In the background field gauge formulation we separate the field as $X_a = \tilde{\alpha} D_a + Q_a$. The action is invariant under $D_a \rightarrow D_a, Q_a \rightarrow U Q_a U^\dagger + U[D_a, U^\dagger]$.

Following the standard Faddeev-Popov procedure [31] and taking the background field configuration to be $D_a = \phi L_a$ one finds, keeping m^2 fixed as the $N \rightarrow \infty$ limit is taken, that $F = -\ln Z$ is given by

$$\frac{F}{N^2} = \frac{3}{4} \log \tilde{\alpha}^4 + \frac{\tilde{\alpha}^4}{2} \left[\frac{\phi^4}{4} - \frac{\phi^3}{3} + m^2 \frac{\phi^4}{4} - \mu \frac{\phi^2}{2} \right] + \log \tilde{\alpha} \phi, \quad (3.9)$$

with $\mu = m^2 - \frac{\rho}{2\sqrt{c_2}}$.

The most notable feature of this expression is that the entire fluctuation contribution is summarized in the logarithmic term $\log(\tilde{\alpha}\phi)$. From (3.9) we see that the effective potential for the order parameter ϕ is

$$\frac{V_{\text{eff}}}{2c_2} = \tilde{\alpha}^4 \left[\frac{\phi^4}{4} - \frac{\phi^3}{3} + m^2 \frac{\phi^4}{4} - \mu \frac{\phi^2}{2} \right] + \log \phi^2 \quad (3.10)$$

The effective potential is not bounded below at $\phi = 0$ due to the $\ln \phi$ term. However, our analysis assumes the existence of a fuzzy sphere ground state and so the effective potential can only be trusted in this phase. It has a local minimum for ϕ positive and sufficiently large $\tilde{\alpha}$ and in this regime the fuzzy sphere configuration exists, for lower values of $\tilde{\alpha}$ our numerical study indicates that the model is indeed in a different phase.

Setting $\phi \frac{\partial F}{\partial \phi} = 0$ (or equivalently $\phi \frac{\partial V_{\text{eff}}(\phi)}{\partial \phi} = 0$) gives

$$\frac{\tilde{\alpha}^4}{2} \left[\phi^4 - \phi^3 + m^2 \phi^4 - \mu \phi^2 \right] + 1 = 0, \quad (3.11)$$

the solution of which specifies ϕ . We define the average of the action, which will be one of the principal observables of our numerical study, as

$$\mathcal{S} = \langle S \rangle / N^2 = \tilde{\alpha}^4 \frac{d}{d\tilde{\alpha}^4} \left(\frac{F}{N^2} \right). \quad (3.12)$$

Then a direct computation and use of eq. (3.11) yields

$$\mathcal{S} = \frac{3}{4} - \frac{\tilde{\alpha}^4 \phi^3}{24} - \frac{\tilde{\alpha}^4 \mu \phi^2}{8}. \quad (3.13)$$

We can also compute the expected radius of the sphere

$$\frac{1}{R} = \frac{\langle Tr D_a^2 \rangle}{N c_2} = -\frac{2}{\tilde{\alpha}^4} \frac{dF}{d\mu} = \phi^2 \quad (3.14)$$

This can also be calculated directly in perturbation theory as

$$\frac{1}{R} = \phi^2 + \frac{1}{c_2 \tilde{\alpha}^4 \phi^2} Tr_3 Tr_{N^2} \left(\frac{1}{\mathcal{L}_c^2 \delta_{ab} + 4m^2 x_a x_b} \right). \quad (3.15)$$

Hence, we conclude that the expected inverse radius of the fuzzy sphere is given by

$$\frac{1}{R} = \phi^2. \quad (3.16)$$

Also

$$\frac{\langle Tr((D_a^2)^2) \rangle}{2N^3 c_2} = \frac{1}{\tilde{\alpha}^4} \frac{\partial}{\partial m^2} \left(\frac{F}{N^2} \right) = \frac{\phi^4}{8}, \quad (3.17)$$

which yields

$$\frac{\langle Tr(D_a^2)^2 \rangle}{2N^3 c_2} = \frac{\phi^4}{8}. \quad (3.18)$$

Scaling $(D_a)_{ij}$ to $(1 - \epsilon)(D_a)_{ij}$ in both the action and measure amounts to a simple coordinate transformation which leaves the partition function invariant. However it also leads to the nontrivial identity

$$\frac{\tilde{\alpha}^4}{N} \langle K_m \rangle = 3N^2, \quad K_m = Tr \left(-[D_a, D_b]^2 + 2i\epsilon_{abc} D_a D_b D_c - 2m^2 D_a^2 + \frac{2m^2}{c_2} (D_a^2)^2 \right). \quad (3.19)$$

Using this identity we can express

$$\mathcal{S} = \frac{3}{4} + \frac{\tilde{\alpha}^4}{6N^3} \langle i\epsilon_{abc} Tr D_a D_b D_c \rangle - \frac{\tilde{\alpha}^4}{2N^3} m^2 \langle Tr D_a^2 \rangle. \quad (3.20)$$

or equivalently in the form

$$\mathcal{S} = 1 + \frac{\tilde{\alpha}^4}{12N^3} \langle Tr[D_a, D_b]^2 \rangle - \frac{\tilde{\alpha}^4}{3N^3} m^2 \langle Tr D_a^2 \rangle - \frac{\tilde{\alpha}^4}{6N^3 c_2} m^2 \langle Tr(D_a^2)^2 \rangle. \quad (3.21)$$

We define the Yang-Mills and Chern-Simons actions by

$$4\text{YM} = -\frac{\langle \text{Tr}[D_a, D_b]^2 \rangle}{2Nc_2}, \quad \text{and } 3\text{CS} = \frac{\langle i\epsilon_{abc} \text{Tr} D_a D_b D_c \rangle}{Nc_2}. \quad (3.22)$$

Then using the above results we find

$$4\text{YM} = \phi^4 + \frac{8}{\tilde{\alpha}^4} \text{ and } 3\text{CS} = -\phi^3. \quad (3.23)$$

In the above we have extensively used the fact that ϕ must satisfy (3.11) and taken $\rho = 0$ i.e. $\mu = m^2$.

Another significant observable for our numerical study is the specific heat C_v defined as

$$C_v := \frac{\langle S^2 \rangle - \langle S \rangle^2}{N^2} = \frac{\langle S \rangle}{N^2} - \tilde{\alpha}^4 \frac{d}{d\tilde{\alpha}^4} \left(\frac{\langle S \rangle}{N^2} \right). \quad (3.24)$$

A direct calculation yields

$$C_v = \frac{3}{4} + \frac{\tilde{\alpha}^5 \phi}{32} (\phi + 2m^2) \frac{d\phi}{d\tilde{\alpha}^4}. \quad (3.25)$$

Finally one can recover perturbation theory in the coupling $g^2 = 1/\tilde{\alpha}^4$ by expanding in $1/\tilde{\alpha}^4$. In particular the one-loop predictions are obtained by using the solution of (3.11) expanded to first order which is $\tilde{\alpha} \rightarrow \infty$ given by

$$\phi = 1 - \frac{2}{1 + 2m^2} \frac{1}{\tilde{\alpha}^4} + O\left(\frac{1}{\tilde{\alpha}^8}\right). \quad (3.26)$$

In the next section we will look at the solution of (3.11) in more detail and the consequences for the transition.

3.4 Phase transitions

Let us now examine the predictions for the quantum transition as determined by F given in (3.9) or the effective potential (3.10) which we repeat here for convenience

$$\frac{V_{\text{eff}}}{2c_2} = \tilde{\alpha}^4 \left[\frac{\phi^4}{4} - \frac{\phi^3}{3} + m^2 \frac{\phi^4}{4} - \mu \frac{\phi^2}{2} \right] + \log \tilde{\phi}^2. \quad (3.27)$$

But first let us review the classical case. The only difference between the full quantum potential (3.10) and the corresponding classical potential is the quantum induced logarithm of ϕ , which as we will see plays a crucial role. The extrema of the classical potential occur at

$$\bar{\phi} = (1 + m^2)\phi = \left\{ 0, \frac{1 - \sqrt{1 + 4t}}{2}, \frac{1 + \sqrt{1 + 4t}}{2} \right\}. \quad (3.28)$$

where $t = \mu(1 + m^2)$. The first and last expressions are local minima and the middle one is the maximum of the barrier between them. For μ positive the global minimum is the third expression, i.e. the largest value of ϕ . When written in terms of $\bar{\phi}$ we see the potential takes the same form as that for $m = 0$ and we can read off that if μ is sent negative then this

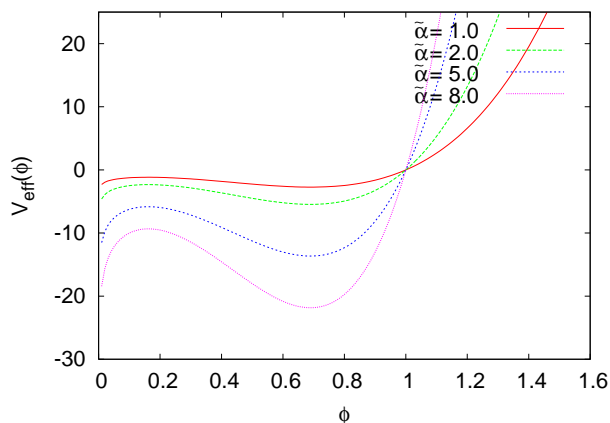


Figure 1. The effective potential for $m^2 = 20$. The minimum corresponds with the fuzzy sphere solution, as we lower the coupling constant the minimum disappears and the fuzzy sphere collapses.

minimum becomes degenerate with that at $\phi = 0$ at $t = \mu(1+m^2) = -\frac{2}{9}$ and the maximum height of the barrier is given by $\frac{\tilde{\alpha}^4}{324(1+m^2)^3}$. When $\mu = m^2$ the minimum is clearly $\phi = 1$, i.e. $D_a = L_a$ for all m and this is separated from the local minimum at $\phi = 0$ by a barrier. The classical transition therefore has the same character as that of the $m = 0$ model and the transition is 1st order and occurs only when ρ is tuned to a critical value.

Let us now consider the effect of the fluctuation induced logarithm of ϕ . The potential is plotted in figure 1 for different values of $\tilde{\alpha}$ and $\mu = m^2 = 20$. The condition $V'_{\text{eff}}(\phi) = 0$ gives us extrema of the model. For large enough $\tilde{\alpha}$ (or low enough temperature) and large enough m and μ it admits four real solutions two for positive ϕ and two for negative ϕ . The largest of the positive ϕ solutions can be identified with the least free energy and therefore the ground state of the system in this phase of the theory. It will determine the actual radius of the sphere. The second positive solution is the local maximum (figure 1) of $V_{\text{eff}}(\phi)$ and will determine the height of the barrier in the effective potential. As the coupling is decreased (or the temperature increased) these two solutions merge and the barrier disappears. This is the critical point of the model and it has no classical counterpart since, in the classical case, the barrier between the two minima never disappears. For smaller couplings than this critical coupling $\tilde{\alpha}_*$ the fuzzy sphere solution $D_a = \phi L_a$ no longer exists and the effective potential cannot be relied on. This is in accord with our numerical simulations which indicate that as the matrix size is increased the radius as defined in (3.14) appears to go to zero.

The condition when the barrier disappears is

$$V''_{\text{eff}} = \frac{\tilde{\alpha}^4}{2} [3\phi^2 - 2\phi + 3m^2\phi^2 - \mu] - \frac{1}{\phi^2} = 0. \tag{3.29}$$

Solving both (3.11) and (3.29) yields $4(1 + m^2)\phi_*^2 - 3\phi_* - 2\mu = 0$ and therefore the

critical values

$$\bar{\phi}_* = \frac{3}{8} \left(1 + \sqrt{1 + \frac{32t}{9}} \right). \tag{3.30}$$

$$g_*^2 = \frac{1}{\tilde{\alpha}_*^4} = \frac{\phi_*^2(\phi_* + 2\mu)}{8}. \tag{3.31}$$

where as defined earlier $\bar{\phi}_* = \phi/(1 + m^2)$ and $t = \mu(1 + m^2)$. Setting both $m^2 = 0$ and $\mu = 0$ yields

$$\phi_* = \frac{3}{4}, \quad \tilde{\alpha}_*^4 = \left(\frac{8}{3} \right)^3. \tag{3.32}$$

while setting $m = 0$ alone leads to no significant simplification and we still have $\phi_* = \bar{\phi}_*$ with $t = \mu$.

If we take μ negative as in the discussion of the last section we see that g_* goes to zero at $t = -1/4$ and the critical coupling $\tilde{\alpha}_*$ is sent to infinity and therefore for $t < -1/4$ the model has no fuzzy sphere phase. This case arises when

$$\rho > 2\sqrt{c_2} \left(m^2 + \frac{1}{4(1 + m^2)} \right). \tag{3.33}$$

However, in the region $-1/4 < \mu < -2/9$ the action (3.6) is completely positive. It is therefore not sufficient to consider only the configuration $D_a = \phi L_a$, but rather all SU(2) representations must be considered. Furthermore for large $\tilde{\alpha}$ the ground state will be dominated by those representations with the smallest Casimir. This means that there is no fuzzy sphere solution for $\mu < -2/9$. A result that we also observe in simulations and in agreement with the result of [30]. We therefore see that the classical transition described above is significantly affected by fluctuations and in particular the fuzzy sphere phase disappears when ρ is increased to the special value of $\frac{4\sqrt{c_2}}{9}$.

The other limit of interest is the limit $\mu = m^2 \rightarrow \infty$. In this case

$$\phi_* = \frac{1}{\sqrt{2}}, \quad \tilde{\alpha}_*^4 = \frac{8}{m^2}. \tag{3.34}$$

This means that the phase transition is located at a smaller value of the coupling constant $\tilde{\alpha}$ as m is increased. In other words the region where the fuzzy sphere is stable is extended to lower values of the coupling or higher temperatures. These results agree nicely with numerical data.

As we cross the critical value of $\tilde{\alpha}$, a rather exotic phase transition occurs where the geometry disappears as the temperature is increased. The fuzzy sphere phase has the background geometry of a two dimensional spherical non-commutative manifold which macroscopically becomes a standard commutative sphere for $N \rightarrow \infty$. The fluctuations are then of a U(1) gauge theory which mixes with a scalar field on this background. In the high temperature phase, which we call a matrix phase, the order parameter ϕ is not well defined and the fluctuations are around diagonal matrices so the model is a pure matrix one corresponding to a zero dimensional Yang-Mills theory in the large N limit. The fuzzy sphere phase occurs for $\tilde{\alpha} > \tilde{\alpha}_*$ while the matrix phase occurs for $\tilde{\alpha} < \tilde{\alpha}_*$.

3.5 Predictions from the effective potential

Since $\phi = 0$ is not a solution of equation (3.11) the extremal equation can be rearranged and when expressed in terms of $\bar{\phi}$ takes the form

$$P(\bar{\phi}) \equiv \bar{\phi}^4 - \bar{\phi}^3 - t\bar{\phi}^2 + \frac{2}{a^4} = 0. \quad (3.35)$$

where $a^4 = \tilde{\alpha}^4/(1+m^2)^3$. By the substitution $\bar{\phi} = (1-4x)\tilde{\phi} + x$, $P(\bar{\phi})$ can be brought to the form of a

$$\tilde{\phi}^4 - \tilde{\phi}^3 - \lambda\tilde{\phi} + \frac{2}{\tilde{\beta}^4} = 0. \quad (3.36)$$

The new parameters λ and $\tilde{\beta}$ are given by

$$\lambda = \frac{x}{(1-4x)^3} \left[x + \frac{4t}{3} \right], \quad (3.37)$$

$$\frac{2}{\tilde{\beta}^4} = \frac{1}{(1-4x)^4} \left[\frac{2(1+m^2)^3}{\tilde{\alpha}^4} - \frac{1}{4} \left(x + \frac{m^2(1+m^2)}{3} \right) \left(x + \frac{5m^2(1+m^2)}{3} \right) \right], \quad (3.38)$$

and the shift x must take one of the two values

$$x \longrightarrow x_{\pm} = \frac{1}{4} \left(1 \pm \sqrt{1 + \frac{8t}{3}} \right). \quad (3.39)$$

We choose $x = x_-$ since $x_-(0) = 0$ and so this case allows us to easily recover the case with $\mu = m^2 = 0$ and for $m^2 \rightarrow 0$ we get

$$x_- = -\frac{m^2}{3} + O(m^4), \quad \lambda = O(m^4), \quad \frac{2}{\tilde{\beta}^4} = \frac{2}{\tilde{\alpha}^4} \left(1 - \frac{7}{3}m^2 + O(m^4) \right) \quad (3.40)$$

The two positive solutions of (3.35), $\bar{\phi}_{\pm}$, for general values of m^2 and μ are then given by

$$\begin{aligned} (1+m^2)\phi_{\pm} &= \frac{1}{4} \left[1 + (1-4x)\sqrt{1+\delta} \pm (1-4x)\sqrt{2-\delta + \frac{2}{\sqrt{1+\delta}}(1+8\lambda)} \right] \\ \delta &= 4W^{\frac{1}{3}} \left[\left(1 + \sqrt{1-V} \right)^{\frac{1}{3}} + \left(1 - \sqrt{1-V} \right)^{\frac{1}{3}} \right] \\ V &= \frac{1}{W^2} \left(\frac{8}{3\tilde{\beta}^4} - \frac{\lambda}{3} \right)^3, \quad W = \frac{1}{\tilde{\beta}^4} + \frac{\lambda^2}{2}. \end{aligned} \quad (3.41)$$

We rewrite the above solution (3.41) as follows, (collecting definitions here for completeness)

$$\begin{aligned} t &= \mu(m^2 + 1), & a^4 &= \frac{\tilde{\alpha}^4}{(1+m^2)^3} \\ q &= 1 + \frac{8t}{3} - \frac{a^4 t^3}{27}, & p &= q^2 - \frac{\left(\frac{8}{3} + \frac{a^4 t^2}{9} \right)^3}{a^4}. \end{aligned} \quad (3.42)$$

Then we can show that

$$(1 - 4x)^3(1 + 8\lambda) = 1 + 4t, \quad W = \frac{q}{(1 + \frac{8t}{3})^3 a^4}, \quad V = 1 - \frac{p}{q^2}. \quad (3.43)$$

and

$$\delta = \frac{4d}{1 + \frac{8t}{3}}, \quad d = a^{-\frac{4}{3}} \left((q + \sqrt{p})^{\frac{1}{3}} + (q - \sqrt{p})^{\frac{1}{3}} \right). \quad (3.44)$$

Substituting one finds the relatively simple form

$$\bar{\phi}_{\pm} = (1 + m^2)\phi_{\pm} = \frac{1}{4} + \frac{1}{2} \sqrt{\frac{1}{4} + \frac{2t}{3} + d} \pm \frac{1}{2} \sqrt{\frac{1}{2} + \frac{4t}{3} - d + \frac{1 + 4t}{4\sqrt{\frac{1}{4} + \frac{2t}{3} + d}}}. \quad (3.45)$$

For completeness the remaining two solutions of the quartic $P(\bar{\phi}) = 0$ are given by

$$\bar{\phi}_{\pm}^n = (1 + m^2)\phi_{\pm}^n = \frac{1}{4} - \frac{1}{2} \sqrt{\frac{1}{4} + \frac{2t}{3} + d} \pm \frac{1}{2} \sqrt{\frac{1}{2} + \frac{4t}{3} - d - \frac{1 + 4t}{4\sqrt{\frac{1}{4} + \frac{2t}{3} + d}}}. \quad (3.46)$$

At the critical point $a = a_c$, p becomes zero and the two solutions $\bar{\phi}_+$ and $\bar{\phi}_-$ are equal.

In the fuzzy sphere phase the ground state of the system is given by ϕ_+ and the barrier maximum is at ϕ_- . The minimum ϕ_+ together with the powers ϕ_+^2 , ϕ_+^3 and ϕ_+^4 are plotted in figures 2 and 3 for $m^2 = 0$ and 200.

In the specific heat we will need the derivative of the minimum with respect to $\tilde{\alpha}$. This is given by

$$\frac{d\bar{\phi}_-}{d\tilde{\alpha}} = \frac{1}{4} \frac{dd}{d\tilde{\alpha}} \left[-\frac{1 + 4t}{8} \frac{1}{\sqrt{\frac{1}{2} + \frac{4t}{3} - d + \frac{1 + 4t}{4\sqrt{\frac{1}{4} + \frac{2t}{3} + d}}} \frac{1}{(\frac{1}{4} + \frac{2t}{3} + d)^{\frac{3}{2}}} \right. \\ \left. - \frac{1}{\sqrt{\frac{1}{2} + \frac{4t}{3} - d + \frac{1 + 4t}{4\sqrt{\frac{1}{4} + \frac{2t}{3} + d}}} + \frac{1}{\sqrt{\frac{1}{4} + \frac{2t}{3} + d}} \right]. \quad (3.47)$$

$$\frac{dd}{d\tilde{\alpha}} = -\frac{4(1 + m^2)^3 a^{\frac{8}{3}}}{3\tilde{\alpha}^5} \left[1 + \frac{8t}{3} + \frac{(1 + \frac{8t}{3})q}{\sqrt{p}} - \frac{4\left(\frac{8}{3} + \frac{t^2 a^4}{9}\right)^2}{a^4 \sqrt{p}} \right] \frac{1}{(q + \sqrt{p})^{\frac{2}{3}}} \\ - \frac{4(1 + m^2)^3 a^{\frac{8}{3}}}{3\tilde{\alpha}^5} \left[1 + \frac{8t}{3} - \frac{(1 + \frac{8t}{3})q}{\sqrt{p}} + \frac{4\left(\frac{8}{3} + \frac{t^2 a^4}{9}\right)^2}{a^4 \sqrt{p}} \right] \frac{1}{(q - \sqrt{p})^{\frac{2}{3}}}. \quad (3.48)$$

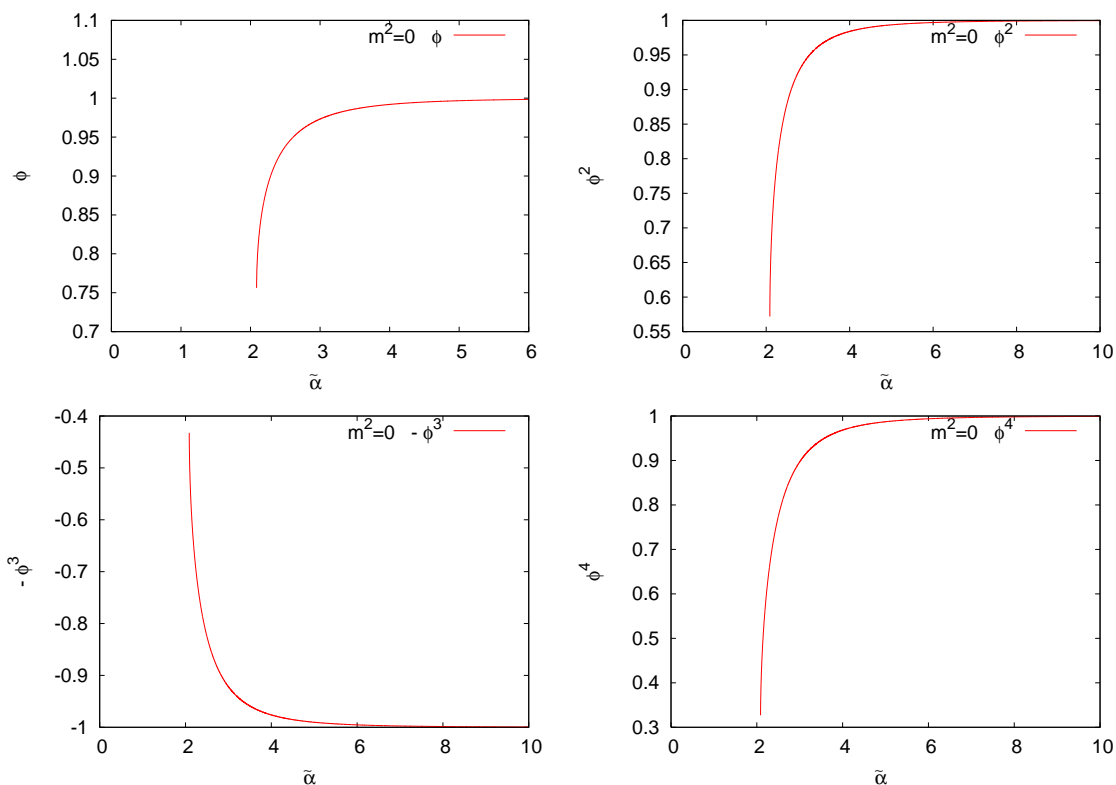


Figure 2. The functions ϕ , ϕ^2 , $-\phi^3$ and ϕ^4 for $m^2 = 0$. ϕ corresponds with ϕ_+ ; the minimum of the effective potential (eq. 3.27).

3.6 Critical behaviour

For $\mu = m^2 = 0$ we have $x = x_- = 0$ and $\lambda = 0$ and the solution

$$\begin{aligned} \phi_+ = \tilde{\phi}_+ = \bar{\phi}_+ &= \frac{1}{4} \left[1 + \sqrt{1 + \delta} + \sqrt{2 - \delta + \frac{2}{\sqrt{1 + \delta}}} \right] \\ \delta &= \frac{4}{\tilde{\alpha}_*^{\frac{4}{3}}} \left[\left(1 + \sqrt{1 - \frac{\tilde{\alpha}_*^4}{\tilde{\alpha}^4}} \right)^{\frac{1}{3}} + \left(1 - \sqrt{1 - \frac{\tilde{\alpha}_*^4}{\tilde{\alpha}^4}} \right)^{\frac{1}{3}} \right] \\ \tilde{\alpha}_*^4 &= \left(\frac{8}{3} \right)^3. \end{aligned} \tag{3.49}$$

Expanding near the critical point we have $\delta = 3 - \frac{16}{3}\epsilon + O(\epsilon^2)$ and we obtain thus the expression

$$\phi = \frac{1}{4} \left[3 + \sqrt{6\epsilon} - \frac{4\epsilon}{3} + O(\epsilon^{\frac{3}{2}}) \right], \quad \epsilon = \frac{\tilde{\alpha} - \tilde{\alpha}_*}{\tilde{\alpha}_*}. \tag{3.50}$$

Substituting into (3.13) near the critical point we obtain the expression for the scaled average action

$$\mathcal{S} = \frac{5}{12} - \frac{1}{3^{\frac{1}{8}} 2^{\frac{5}{8}}} \sqrt{\tilde{\alpha} - \tilde{\alpha}_*} - \frac{7}{3^{\frac{5}{4}} 2^{\frac{5}{4}}} (\tilde{\alpha} - \tilde{\alpha}_*) + O\left((\tilde{\alpha} - \tilde{\alpha}_*)^{\frac{3}{2}} \right), \tag{3.51}$$

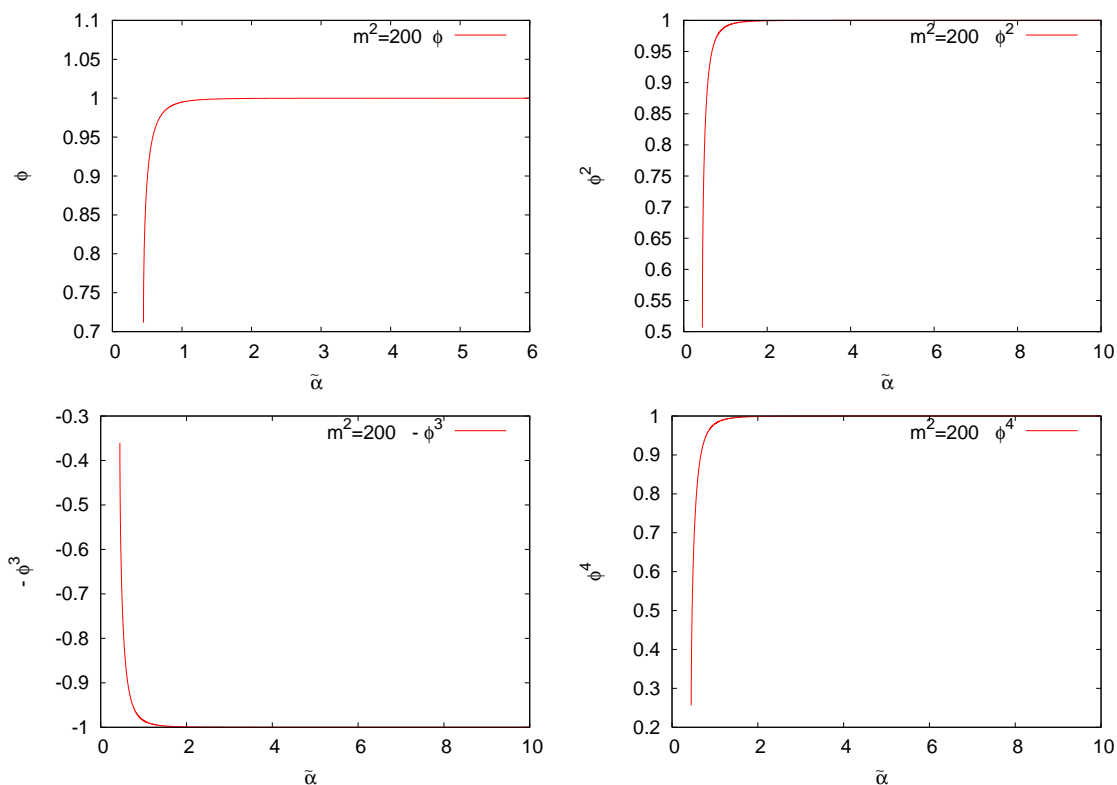


Figure 3. The functions ϕ , ϕ^2 , $-\phi^3$ and ϕ^4 for $m^2 = 200$.

and the specific heat is then given by

$$C_v = \frac{29}{36} + \frac{1}{2^{\frac{11}{8}} 3^{\frac{7}{8}}} \frac{1}{\sqrt{\tilde{\alpha} - \tilde{\alpha}_*}} + O\left((\tilde{\alpha} - \tilde{\alpha}_*)^{\frac{1}{2}}\right). \quad (3.52)$$

This gives a divergent specific heat with critical exponent

$$\alpha = \frac{1}{2}. \quad (3.53)$$

If instead we consider $\mu = 0$ but $m \neq 0$ so that $t = 0$ then the above expressions remain essentially the same provided we substitute a for $\tilde{\alpha}$. The critical behaviour remains the same for this case with the critical inverse temperature

$$\beta_c = \tilde{\alpha}_*^4 = \left(\frac{8}{3}\right)^3 (1 + m^2)^3, \quad (3.54)$$

so that increasing m^2 with $\mu = 0$ sends the critical temperature lower and so the region of stability of the fuzzy sphere solution is reduced.

3.7 The generic case

At the critical point the coupling a takes the value a_* and the order parameter ϕ takes the value ϕ_* . At this critical point the two solutions ϕ_+ and ϕ_- merge. This is more easily

determined by requiring the additional equation

$$\frac{2(1+m^2)^3}{\tilde{\alpha}^4} \phi^2 \frac{d^2 V_{\text{eff}}}{d\phi^2} = Q(\bar{\phi}) \equiv 3\bar{\phi}^4 - 2\bar{\phi}^3 - t\bar{\phi}^2 - \frac{2}{a^4} = 0. \quad (3.55)$$

Putting the two equations $P(\bar{\phi}) = 0$ and $Q(\bar{\phi}) = 0$ together we obtain

$$P(\bar{\phi}) + Q(\bar{\phi}) = 4\bar{\phi}^4 - 3\bar{\phi}^3 - 2t\bar{\phi}^2 = \bar{\phi} \frac{dP(\bar{\phi})}{d\bar{\phi}}. \quad (3.56)$$

In other words $\frac{dP(\bar{\phi})}{d\bar{\phi}} = 0$ at the critical point. Expanding around the critical

$$\bar{\phi} = \bar{\phi}_* + \sigma. \quad (3.57)$$

and using $P(\bar{\phi}_*) = P'(\bar{\phi}_*) = 0$ we obtain

$$P(\bar{\phi}) = \sigma^4 + (4\bar{\phi}_* - 1)\sigma^3 + \frac{3\bar{\phi}_* + 4t}{2}\sigma^2 + \frac{2}{a^4} - \frac{2}{a_*^4} = 0. \quad (3.58)$$

For small σ , treating σ^4 and σ^3 perturbatively we get

$$\begin{aligned} \sigma &= \sqrt{\frac{2}{3\bar{\phi}_* + 4t} \left(\frac{2}{a_*^4} - \frac{2}{a^4} \right)} - \frac{(4\bar{\phi}_* - 1)}{(3\bar{\phi}_* + 4t)^2} \left(\frac{1}{a_*^4} - \frac{1}{a^4} \right) + \dots \\ &= \frac{4}{a_*^{\frac{5}{2}}} \frac{1}{\sqrt{3\bar{\phi}_* + 4t}} \sqrt{a - a_*} - \frac{(16\bar{\phi}_* - 1)}{a_*^5 (3\bar{\phi}_* + 4t)^2} (a - a_*) + \dots \end{aligned} \quad (3.59)$$

Hence

$$\bar{\phi} = \bar{\phi}_* + \frac{4}{a_*^{\frac{5}{2}}} \frac{1}{\sqrt{3\bar{\phi}_* + 4t}} \sqrt{a - a_*} + \dots \quad (3.60)$$

or equivalently to leading order we have

$$\phi = \phi_* + \frac{4}{\tilde{\alpha}_*^{\frac{5}{2}}} \frac{1}{\sqrt{3\bar{\phi}_* + 4\mu}} \sqrt{\tilde{\alpha} - \tilde{\alpha}_*} + \dots \quad (3.61)$$

The average action \mathcal{S} near the critical point can be computed using this expression of ϕ in equation (3.13). The result is that

$$\mathcal{S} = \mathcal{S}_* - a_c^4 \frac{\bar{\phi}_* (\bar{\phi}_* + 2t)}{\sqrt{3\bar{\phi}_* + 4t}} \sqrt{\frac{a - a_c}{a_c}} + \dots \quad (3.62)$$

Where

$$\mathcal{S}_* = \frac{3}{4} - \frac{(\bar{\phi}_* + 3t)}{3(\bar{\phi}_* + 2t)} \quad (3.63)$$

which interpolates between $\mathcal{S}_* = \frac{5}{12}$ for $t = 0$ and $\mathcal{S}_* = \frac{1}{4}$ for large t .

In order to compute the specific heat we need the derivative

$$\frac{d\phi}{d\tilde{\alpha}} = \frac{2}{\tilde{\alpha}_*^{\frac{5}{2}}} \frac{1}{\sqrt{3\bar{\phi}_* + 4\mu}} \frac{1}{\sqrt{\tilde{\alpha} - \tilde{\alpha}_*}} + \dots \quad (3.64)$$

The divergent term in the specific heat is still given by a square root singularity. From (3.25) we get

$$C_v = C_v^B + \frac{\phi_*(\phi_* + 2\mu)}{16\sqrt{3\phi_* + 4\mu}} \frac{\tilde{\alpha}_*^{\frac{5}{2}}}{\sqrt{\tilde{\alpha} - \tilde{\alpha}_*}} + \dots \quad (3.65)$$

where the background constant contribution to the specific heat C_v^B is given by

$$C_v^B = \frac{3}{4} + \frac{(3 + 4t)\bar{\phi}_* + 2t}{8(3\bar{\phi} + 4t)^2} \quad (3.66)$$

If we set $\mu = 0$ in (3.61) and (3.65) we recover (3.50) and (3.52). Let us recall that the critical value $\tilde{\alpha}_*$ can be given by the formula

$$\tilde{\alpha}_*^4 = \frac{8}{\phi_*^2(\phi_* + 2\mu)}. \quad (3.67)$$

Then (3.65) can be put in the form

$$C_v = C_v^B + \frac{1}{8\sqrt{1 + \frac{\tilde{\alpha}_*^4 \phi_*^3}{16}}} \frac{\sqrt{\tilde{\alpha}_*}}{\sqrt{\tilde{\alpha} - \tilde{\alpha}_*}} + \dots \quad (3.68)$$

The prediction here is that the critical exponent of the specific heat for this model is given precisely by

$$\alpha = \frac{1}{2} \quad (3.69)$$

Specializing to the case $\mu = m^2$ we see the coefficient of the singularity for any small m^2 (i.e the amplitude) is

$$c(m^2) = \frac{\sqrt{\tilde{\alpha}_*}}{8\sqrt{1 + \frac{\tilde{\alpha}_*^4 \phi_*^3}{16}}}. \quad (3.70)$$

If we extrapolate these results to large m^2 where we know that $\phi_* \rightarrow 1/\sqrt{2}$ and $\tilde{\alpha}_*^4 \rightarrow 8/m^2$ we get

$$C_v = \frac{3}{4} + \frac{1}{32\sqrt{2}m^2} + \frac{1}{2^{\frac{21}{8}}m^{\frac{1}{4}}} \frac{1}{\sqrt{\tilde{\alpha} - \tilde{\alpha}_*}} + \dots \quad (3.71)$$

The coefficient of the singularity and the critical value $\tilde{\alpha}_*$ become very small and vanish when $m^2 \rightarrow \infty$. For comparative purposes we can compute the ratio

$$\frac{c(m^2)}{c(0)} = \left[\frac{1}{8} \left(\frac{3}{2} \right)^7 \frac{1}{m^2} \right]^{\frac{1}{8}}. \quad (3.72)$$

For $m^2 = 200$ we get the ratio $c(200)/c(0) = 0.57$ which is not yet very small. As we will see below our data (see figure 12) in the critical region for large m is not precise enough to confirm or rule out the presence of a singularity.

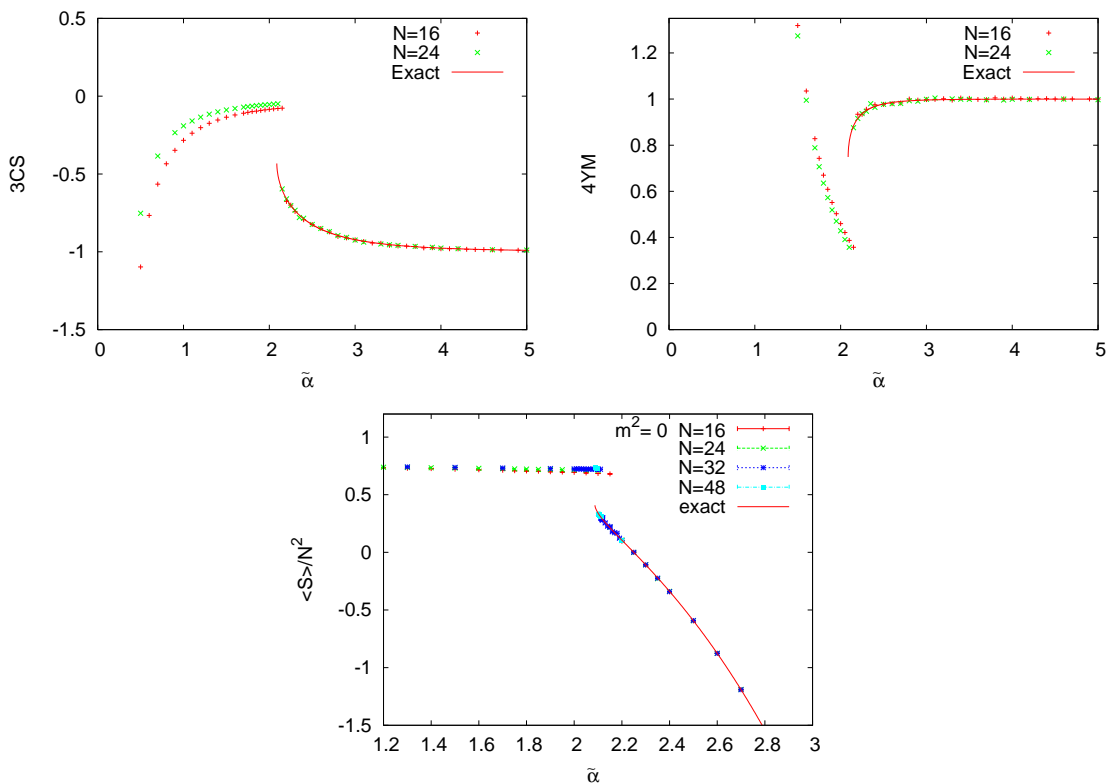


Figure 4. The observables CS , YM and $\frac{\langle S \rangle}{N^2}$ for $m^2 = 0$ as a function of the coupling constant for different matrix sizes N . The solid line corresponds to the theoretical prediction using the local minimum (3.45) of the effective potential.

4 Numerical results

Let us now turn to the numerical simulations. A fully nonperturbative study of this model is done in [7, 15]. For the model with $m^2 = 0$ see also [5, 17]. In Monte Carlo simulations we use the Metropolis algorithm and the action (3.5) with N in the range $N = 8$ to 104 and m^2 in the range $m^2 = 0$ to 1000. The errors were estimated using the binning-jackknife method. We measure the radius of the sphere R (the order parameter) defined by $Nc_2/R = \langle Tr D_a^2 \rangle$, the average value of the action $\langle S \rangle$ and the specific heat $C_v = \frac{\langle (S - \langle S \rangle)^2 \rangle}{N^2}$ as functions of $\tilde{\alpha}$ for different values of N and m^2 . We also measure the eigenvalue distributions of several operators.

4.1 The theory with $m^2 = 0$

For $m^2 = 0$ we observe that the expectation values \mathcal{S} , YM , CS (defined above) are all discontinuous at $\tilde{\alpha}_s = 2.1 \pm 0.1$ (figure 4). This is where the transition occurs. Indeed this agrees with the theoretical value $\tilde{\alpha}_* = 2.087$. The theory also predicts the behaviour of these actions in the fuzzy sphere phase. There clearly exists a latent heat and hence we are dealing with a 1st order transition which terminates at some value of m^2 . The radius is also discontinuous at the critical point (figure 5) whereas the specific heat is discontinuous

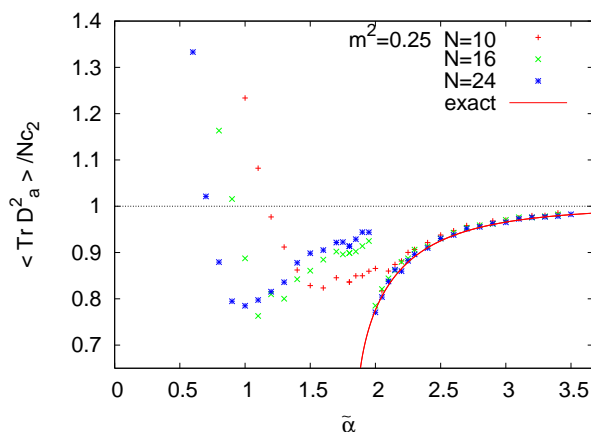


Figure 5. The inverse radius for $m^2 = 0.25$ against $\tilde{\alpha}$ for $N = 10, 16, 24$. The solid line corresponds to ϕ^2 , given by eq. (3.45).

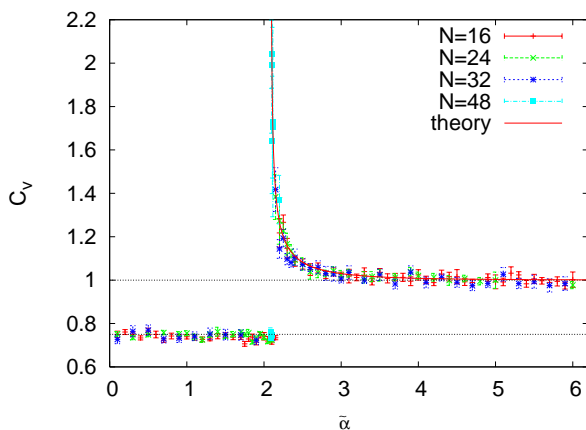


Figure 6. The specific heat for $m^2 = 0$ as a function of the coupling constant for $N = 16, 24, 32, 48$. The curve corresponds with the theoretical prediction given by eq. (3.25) for $m^2 = 0$.

fuzzy sphere ($\tilde{\alpha} > \tilde{\alpha}_*$)	matrix phase ($\tilde{\alpha} < \tilde{\alpha}_*$)
$R = 1$	$R = 0$
$C_v = 1$	$C_v = 0.75$

Table 1. Comparison of the fuzzy sphere phase and the matrix phase.

and divergent (figure 6). Near the critical point we compute a divergent specific heat with critical exponent $\alpha = 1/2$ (equation (3.52)). The fit for data fixing $\alpha = 0.5$ gives the critical value $\tilde{\alpha}_c = 2.125 \pm 0.007$ again with good agreement with the theory. From the matrix side the specific heat seems to be a constant equal to 0.75 and therefore the critical exponent is zero. The inverse radius in the matrix phase goes through a minimum and then rise quickly and sharply to infinity (figure 5).

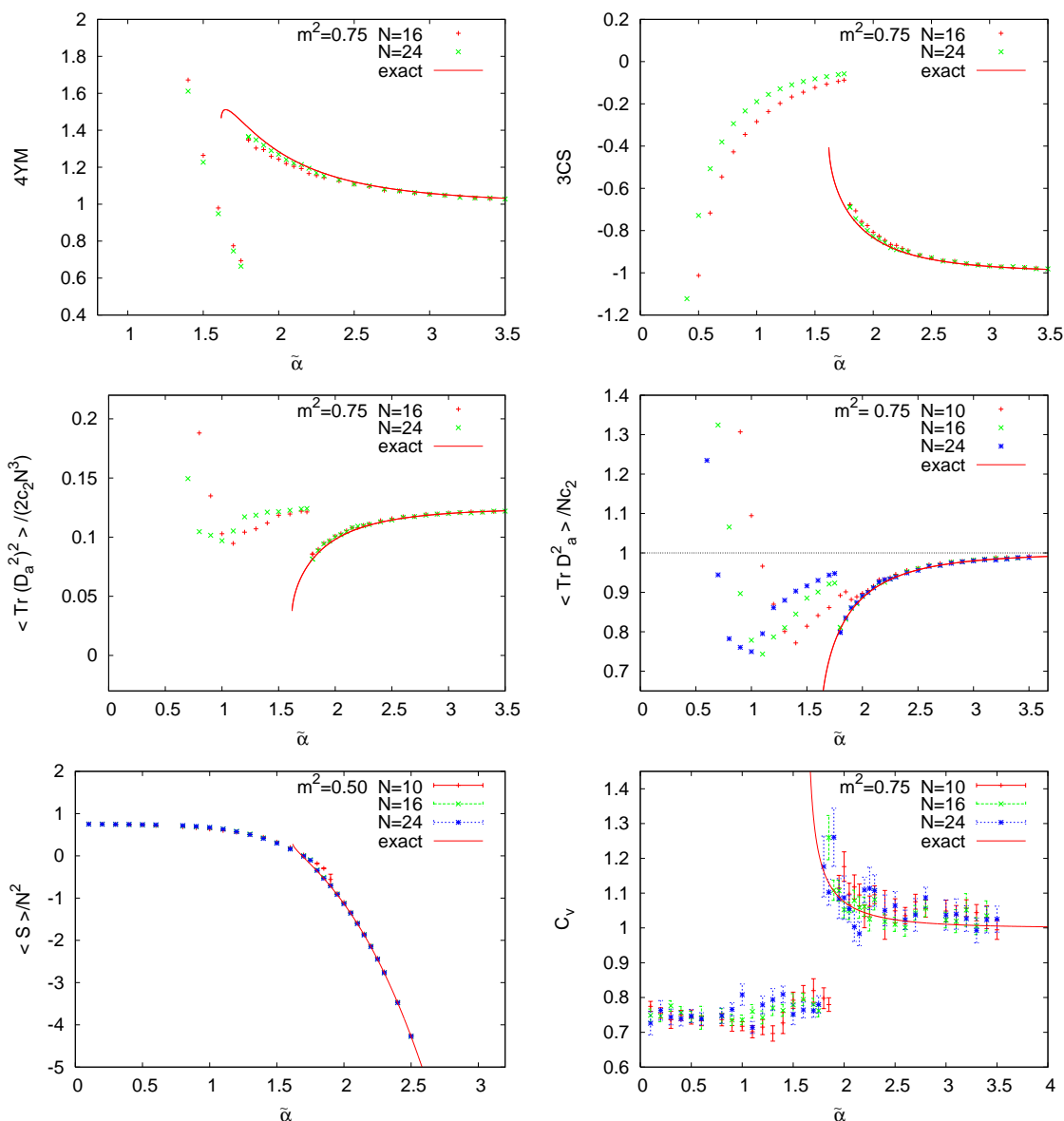


Figure 7. Different observables for $m^2 = 0.75$ plotted against $\tilde{\alpha}$ for different matrix sizes. Again the solid lines represent the theoretical predictions using the local minimum of the effective potential.

4.2 The action, radius and specific heat for $m^2 \neq 0$

For small values of m^2 we determine the critical value $\tilde{\alpha}_s$ as the point of discontinuity in S , YM, CS, $Tr(D_a^2)^2$ and the radius $Tr D_a^2$. This is where the divergence in C_v occurs. For example for $m^2 = 0.75$ the action looks continuous but its parts are all discontinuous with a jump. The radius is also discontinuous with a jump. The specific heat is still divergent in this case (figure 7). This is still 1st order.

For $m^2 = 55$ the action and its parts become continuous. We find in particular that the Chern-Simons and the radius are becoming continuous around $m^2 = 40 - 50$. These

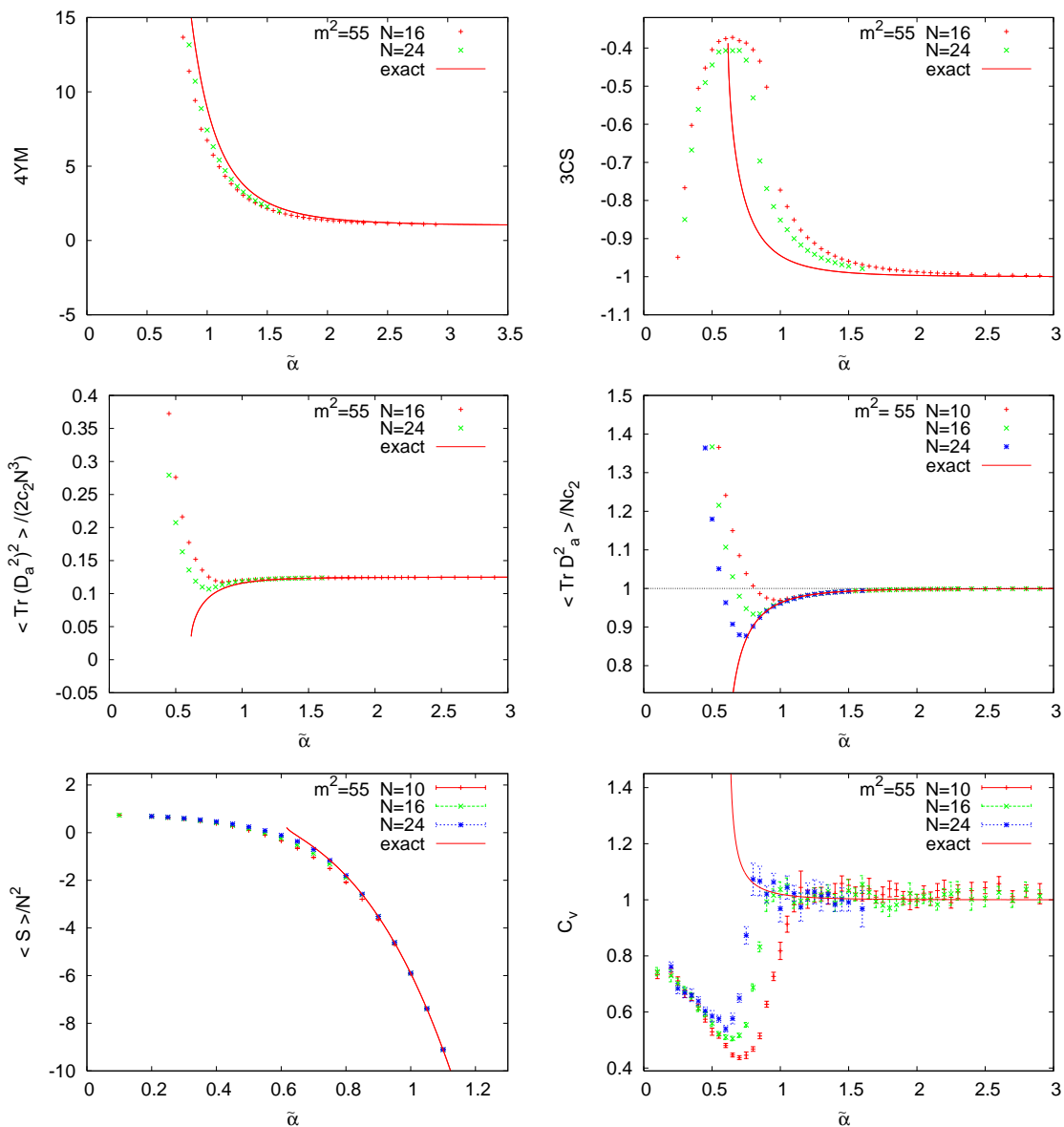


Figure 8. Different observables for $m^2 = 55$ as functions of the coupling constant for different matrix sizes.

are the two operators which are associated with the geometry. The specific heat seems now to be continuous (figure 8). This looks like a 3rd order transition.

4.3 The limit $m^2 \rightarrow \infty$ and specific heat

In this case we measure the critical value $\tilde{\alpha}_s$ as follows. We observe that different actions $\langle S \rangle$ which correspond to different values of N (for some fixed value of m^2) intersect at some value of the coupling constant $\tilde{\alpha}$ which we define $\tilde{\alpha}_s$ (figure 9). This is the critical point. For example we find for $m^2 = 200$ the result $\tilde{\alpha}_s = 0.4 \pm 0.1$. The theoretical value is

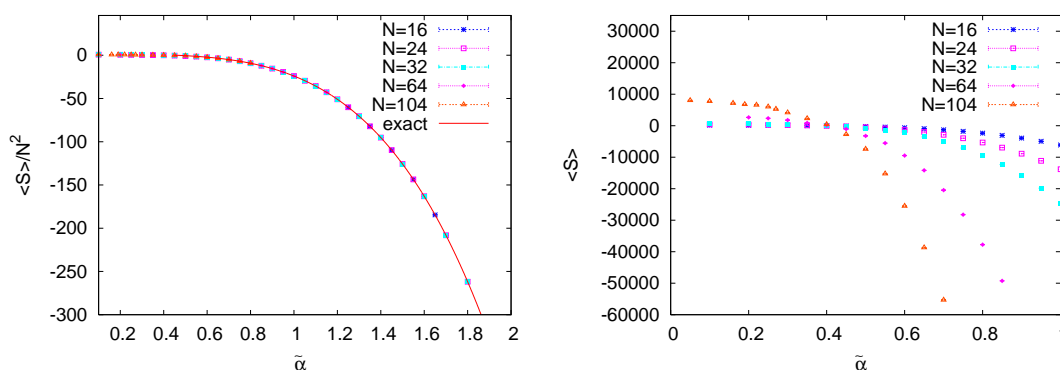


Figure 9. The observables $\frac{\langle S \rangle}{N^2}$ (left) and $\langle S \rangle$ (right) for $m^2 = 200$ plotted as functions of $\tilde{\alpha}$ for $N = 16, 24, 32, 64, 104$. The value of $\tilde{\alpha}$ at which the curves $\langle S \rangle$ for different values of N cross is defined as $\tilde{\alpha}_s$.

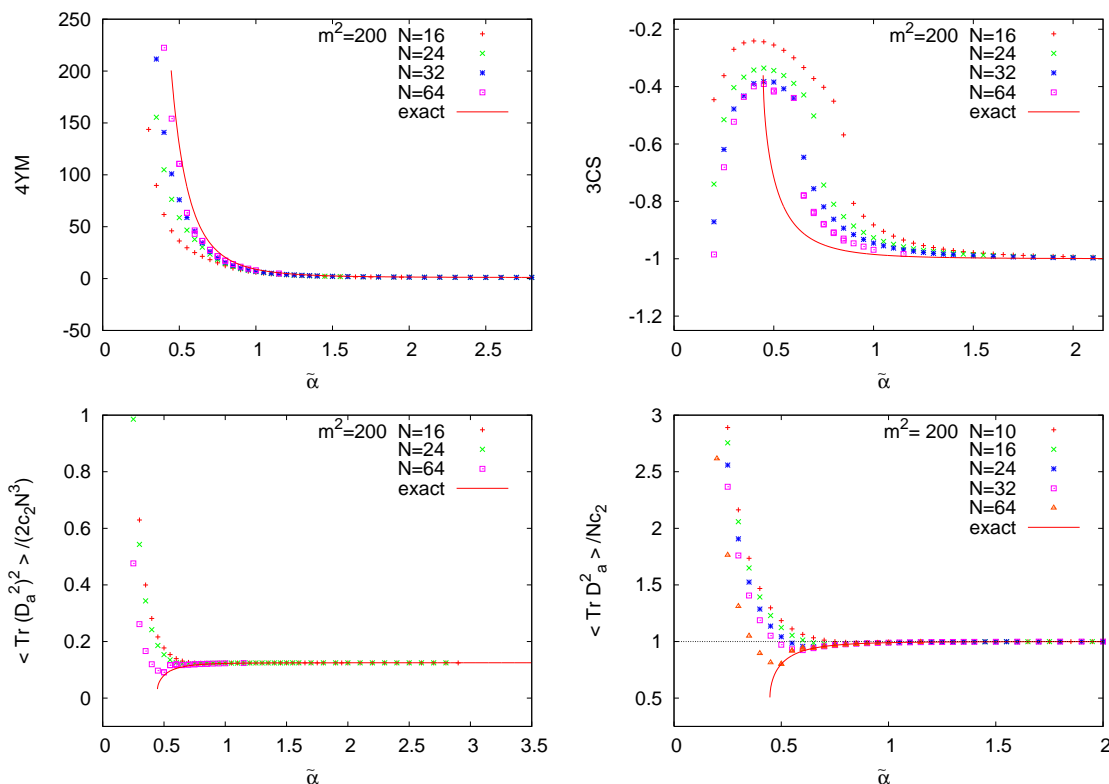


Figure 10. Other observables for $m^2 = 200$ as functions of the coupling constant for $N = 16, 24, 32, 64$. The solid lines correspond to the theoretical predictions. We observe that the data tend to approach the theoretical prediction as N is increased.

$\tilde{\alpha}_* = 0.44$. For large m^2 the theoretical critical value $\tilde{\alpha}_*$ is given by equation (3.34). The measured value $\tilde{\alpha}_s$ tends to be smaller than this predicted value.

The quantities \mathcal{S} , YM, CS, $\langle Tr(D_a^2)^2 \rangle$ and the radius are all continuous across the

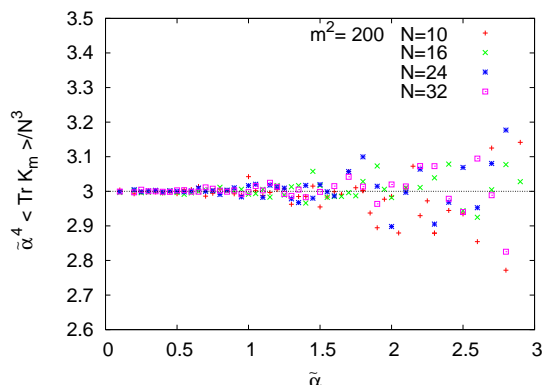


Figure 11. The Ward identity (3.19) for $m^2 = 200$ as a function of the coupling constant $\tilde{\alpha}$ for $N = 10, 16, 24, 32$.

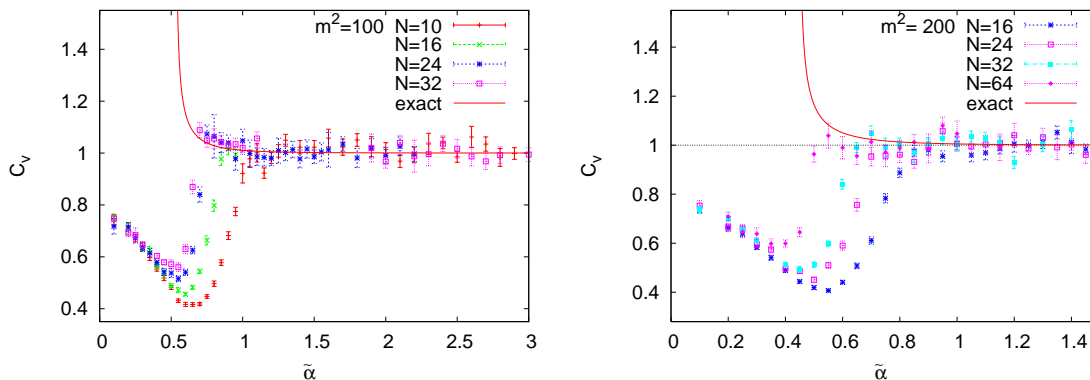


Figure 12. The specific heat for $m^2 = 100$ and 200 for different matrix sizes. In the region of the fuzzy sphere the value of the specific heat is 1. In the region of the matrix phase the value of the specific heat tends to take the constant value 0.75 as the size of matrix N increases.

transition point in this regime (figure 10). We observe that near the critical point the numerical results approach the theoretical curves as we increase N . We also checked the Ward identities (3.19), (3.20) and (3.21) (figure 11).

The specific heat in the fuzzy sphere phase is constant equal to 1, it starts to decrease at $\tilde{\alpha}_{\max}$, goes through a minimum at $\tilde{\alpha}_{\min}$ and then goes up again to the value 0.75 when $\tilde{\alpha} \rightarrow 0$ (figure 12). The values $\tilde{\alpha}_{\max, \min}$ decrease with N while the minimum value of C_v increases. Extrapolating the $\tilde{\alpha}_{\max}$ and $\tilde{\alpha}_{\min}$ to $N = \infty$ (figure 13) we obtain our estimate for the critical coupling $\tilde{\alpha}_c$ which agree with $\tilde{\alpha}_s$ within errors. The matrix-to- S_N^2 phase transition looks then 3rd order. However it could be that for large N the specific heat becomes discontinuous at the critical point with a jump, i.e the transition is discontinuous with 2nd order fluctuations.

Thus it seems that the specific heat in the regime of large values of m^2 is such that *i*) $\tilde{\alpha}_{\max, \min}$ approach $\tilde{\alpha}_s$ in the limit $N \rightarrow \infty$ and *ii*) that the specific heat becomes constant in the matrix phase and equal to $C_v = 0.75$. There remains the question of whether or not the specific heat has critical fluctuations at the critical point for large m^2 .

The theory still predicts a transition (equation (3.65)) with critical fluctuations and

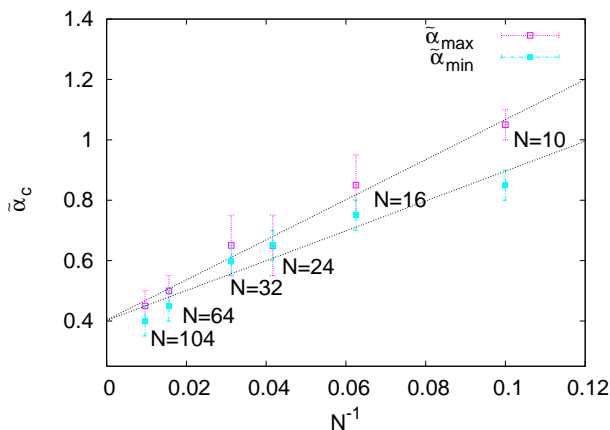


Figure 13. By extrapolating the measured values of $\tilde{\alpha}_{\max}$ and $\tilde{\alpha}_{\min}$ to $N = \infty$ we obtain the critical value $\tilde{\alpha}_c$.

a divergence in the specific heat with a critical exponent $\alpha = 1/2$ and with a very small amplitude (the coefficient of the square root singularity). There is possibly some evidence for this even for $m^2 = 100$ but none for $m^2 = 200$. To resolve this question we need to go very near the critical point and simulate with bigger N .

4.4 The phase diagram

Our phase diagram in terms of the parameters $\tilde{\alpha}$ and m^2 which we have studied is given in figure 14. We have identified two different phases of the matrix model (3.5). In the *geometrical* or *fuzzy sphere phase* we have a $U(1)$ gauge theory on S_N^2 ; the geometry of the sphere and the structure of the $U(1)$ gauge group are stable under quantum fluctuations so the theory in the continuum limit is an ordinary $U(1)$ on the sphere. In the *matrix phase* the fuzzy sphere vacuum collapses under quantum fluctuations and there is no underlying sphere in the continuum large N limit. In this phase the model should be described by a pure matrix model without any background spacetime geometry. The transition in the Ehrenfest classification would be labeled a first order transition, but this classification is not very helpful. The transition described here is a very exotic one with both a latent heat and a divergent specific heat. We know of no other example of such a transition. As we follow this line of transitions the entropy jump or equivalently the latent heat becomes zero at around $m^2 \sim 40$ and remains zero for larger m^2 . Our theoretical analysis indicates that there is still a divergent specific heat, however our numerical simulations are not fine enough to determine whether this is so or not.

For large m^2 the transition (we expect) still has a divergent specific heat as the transition is approached from the fuzzy sphere side. This is the conclusion of our theoretical analysis and our numerical results are consistent with this. But our numerical results are not conclusive. It may also be that the transition is even in Ehrenfest's classification a *3rd* order, where there is a jump in the specific heat with no divergence. We could not determine the nature of the transition in the large m regime with any confidence from the numerical

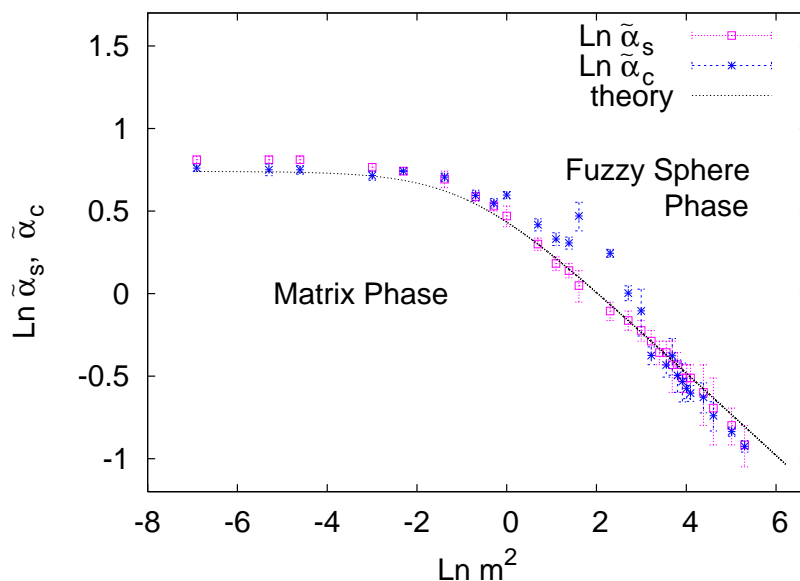


Figure 14. The phase diagram shows the curve separating the geometrical and matrix phases of the model (3.6) with $\mu = m^2$. The critical curve is given by eq. (3.31) and describes (at least for small values of m^2) a line of exotic transition with a jump in the entropy yet with divergent critical fluctuations and a divergent specific heat with critical exponent $\alpha = 0.5$, when approached from the fuzzy sphere side. The points which lay off the critical line in the middle mass region might suggest the existence of a multicritical point.

data. In all cases the fuzzy sphere-to-matrix theory transitions are from a one-cut phase (the matrix phase) to a point or discrete spectrum in the geometrical (fuzzy sphere) phase.

The specific heat in the fuzzy sphere phase takes the value 1 where the gauge field can only contribute the amount 1/2. This can be understood as follows. The high temperature limit of the specific heat for any matrix model is governed by the largest term and must go like $N_{\text{total}}/\text{degree}$ where N_{total} is the total number of degrees of freedom and *degree* is the degree of the polynomial. This gives the limiting high temperature limit of the specific heat be $\frac{3}{4}$ for all values of the parameters. In the simple model with $m = 0$ and $\mu = 0$ this value is achieved from the transition point onwards.

For the full model in the large m^2 regime the effect of the potential V should be dominant. This can be seen by remarking that in the strong-coupling limit $m^2 \rightarrow \infty$, $\tilde{\alpha} \rightarrow 0$ keeping fixed $\tilde{\alpha}^4 m^2$ the action S reduces to V . Note that if we consider V alone with a measure given by $\int [d\Phi']$ (with $\Phi' = \sqrt{D_a^2}$) instead of $\int [dD_a]$ then we will get the usual quartic potential dynamics with a well known 3rd order transition. Here when we consider the model given by the potential V with the measure $\int [dD_a]$ we obtain the specific heat given in figure 15. In the region of parameters corresponding to the matrix phase the specific heat shows in this case a structure similar to that of the full model S . However in the region of parameters corresponding to the fuzzy sphere phase the specific heat is given now by $C_v = 1/2$. Thus the field Φ contributes only the amount 1/2 to C_v . Indeed

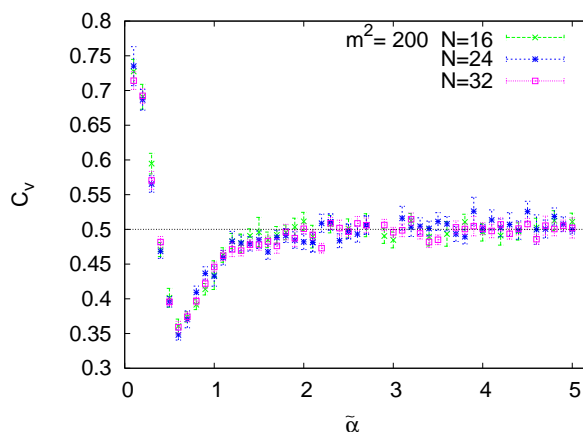


Figure 15. The specific heat for the pure potential with $m^2 = 200$ as function of the coupling constant computed with respect to the Boltzmann weight e^{-V} .

from the eigenvalue distribution of the operator Φ computed in the fuzzy sphere phase it is shown explicitly that Φ has Gaussian fluctuations. The behaviour of C_v in the full model S is thus a non-trivial mixture of the behaviours in S_0 (first order transition) and V (3rd order transition) considered separately.

Given that the behaviour of the full model can be described as a non-trivial mixture of the model S_0 and the potential we expect that the effect of adding the potential to the model is to shift the transition temperature and provide a non-trivial background specific heat. The divergence of the specific heat arises from the interplay of the two terms in S_0 , i.e. between the Chern-Simons and Yang-Mills terms. Given that this competition leads to a divergence of the specific heat it should eventually emerge from the background sufficiently close to the transition.

4.5 The eigenvalue distributions for large m^2

4.5.1 The low temperature phase (fuzzy sphere)

Numerically we can check that the normal scalar field and the tangent gauge field decouple from each other in the “fuzzy sphere phase” in the limit $m^2 \rightarrow \infty$ by computing the eigenvalues of the operators D_a^2 and D_3 . See figure 16. The fit for the distribution of eigenvalues of $D_a^2 - c_2$ is given by the Wigner semi-circle law

$$\rho(x) = \frac{2}{a_{\text{eff}}^2 \pi} \sqrt{a_{\text{eff}}^2 - x^2}. \tag{4.1}$$

This distribution is consistent with the effective Gaussian potential

$$V_{\text{eff}}^{\text{sph}} = \frac{2}{a_{\text{eff}}^2} \text{Tr}(D_a^2 - c_2)^2, \quad a_{\text{eff}}^2 = \frac{4c_2 N}{m^2 \tilde{\alpha}_{\text{eff}}^4}. \tag{4.2}$$

We find numerically table 2. The parameter a is the theoretical prediction given by $a^2 =$

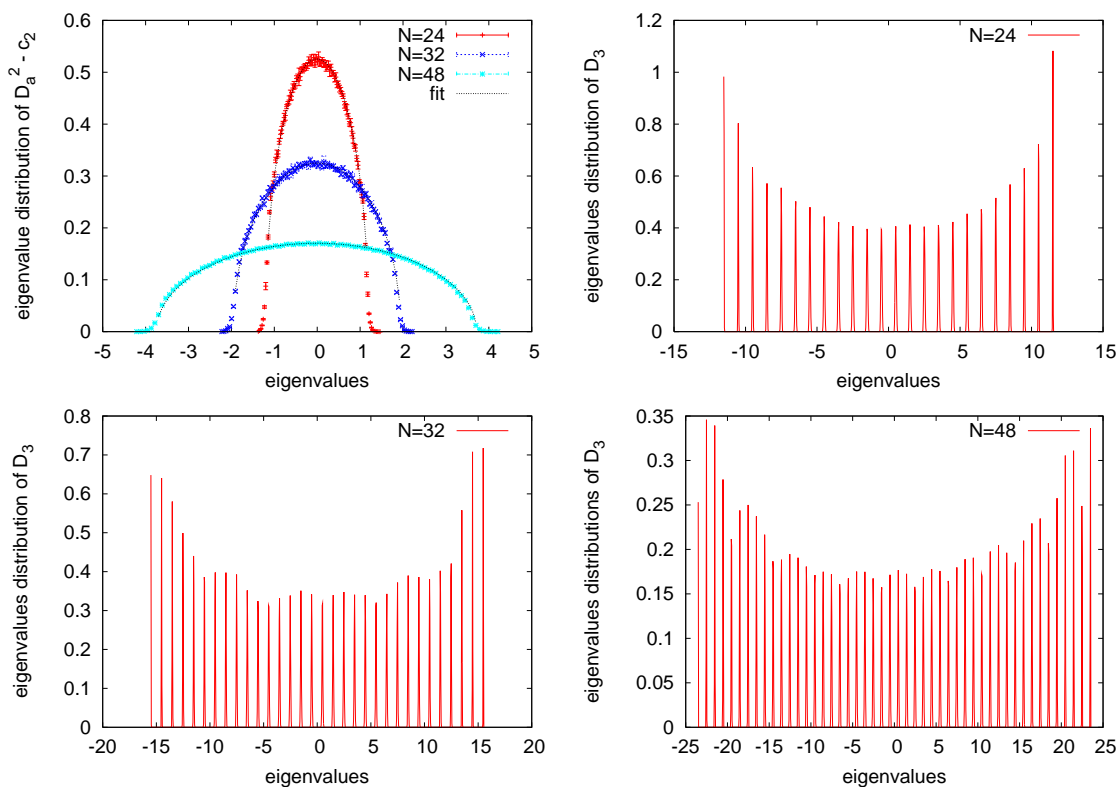


Figure 16. The eigenvalue distribution of $D_a^2 - c_2$ (left) for $N = 24, 32, 48$ and D_3 (right) for $N = 24, N = 32$ and $N = 48$ in the fuzzy sphere phase with $m^2 = 200$ and $\tilde{\alpha} = 5$. The fit for $D_a^2 - c_2$ corresponds with the Wigner semi-circle law (4.1).

N	a_{eff}^2	a^2
24	1.4632 ± 0.0016	0.1104
32	3.8206 ± 0.0068	0.2619
48	13.9886 ± 0.0110	0.8844

Table 2. The measured value and the theoretical prediction of the coupling constant a^2 for $m^2 = 200$ and $\tilde{\alpha} = 5$ for different values of N .

$4c_2 N / m^2 \tilde{\alpha}^4$ which goes like N^3 . The effective parameter a_{eff}^2 is found to behave as

$$a_{\text{eff}}^2 = (3.7645 \pm 0.6557) \times 10^{-5} \times N^{3.3170 \pm 0.0492}. \tag{4.3}$$

This means that the renormalized value $\tilde{\alpha}_{\text{eff}}$ of the gauge coupling constant is slowly decreasing with N . Equivalently the parameter a_{eff} yields a small correction to the classical

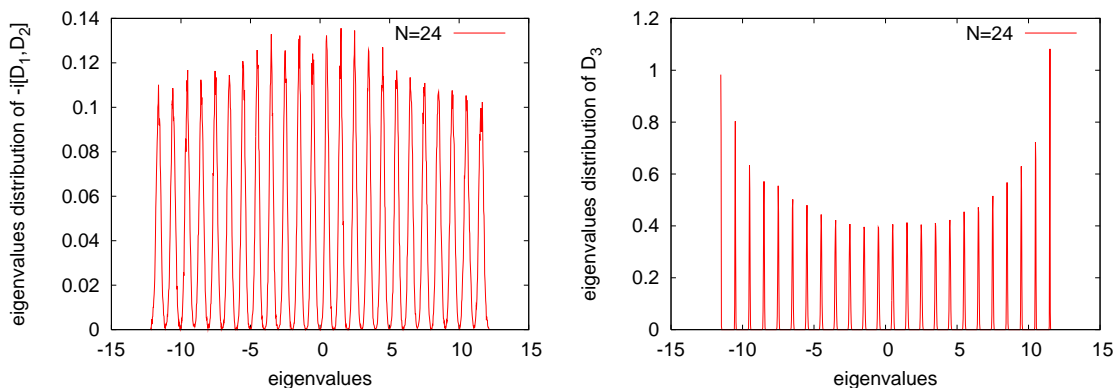


Figure 17. The eigenvalue distributions of $-i[D_1, D_2]$ and D_3 in the fuzzy sphere phase for $m^2 = 200$ and $\tilde{\alpha} = 5$.

potential V which is linear in Φ . Indeed we can show that

$$\begin{aligned}
 Z &= \int dD_a e^{-\frac{2}{a_{\text{eff}}} \text{Tr}(D_a^2 - c_2)^2} \\
 &= e^{C_0} \int dD_a e^{-\frac{2}{a^2} \text{Tr}(D_a^2 - c_2)^2 - \frac{4c_2}{a} \left(\frac{1}{a} - \frac{1}{a_{\text{eff}}}\right) \text{Tr}(D_a^2 - c_2)} \\
 C_0 &= -2Nc_2^2 \left(\frac{1}{a} - \frac{1}{a_{\text{eff}}}\right)^2 - \frac{3}{2}N^2 \log \frac{a}{a_{\text{eff}}}. \tag{4.4}
 \end{aligned}$$

This shows explicitly that having $a_{\text{eff}} \neq a$ means that there is an extra linear term in ϕ added to the classical potential.

In the fuzzy sphere phase the field configurations D_a are thus given by (or are close to) representations of $SU(2)$ of spin $s = \frac{N-1}{2}$ as we can clearly see on figure 16. Indeed the eigenvalues of D_3 for $\tilde{\alpha} = 5$ and $m^2 = 200$ are found to lie within the range $-\frac{N-1}{2}, \dots, 0, \dots, \frac{N-1}{2}$ as expected for $N = 24$ and $N = 32$. The eigenvalues of the commutator $-i[D_1, D_2]$ are also found to lie in the range $-\frac{N-1}{2}, \dots, 0, \dots, \frac{N-1}{2}$ (figure 17).

4.5.2 The high temperature phase (matrix phase)

The distribution of the eigenvalues of D_a^2 suffers a distortion as soon as the system undergoes the matrix-to-sphere transition and deviations from the Wigner semi-circle eigenvalue distribution (4.1) become large as we lower the coupling constant $\tilde{\alpha}$. See figures 18 and 19.

In this phase the distribution for D_3 is symmetric around zero and the fit is given by the one-cut solution

$$\rho(x) = \frac{16}{c(c+4b)} \frac{1}{2\pi} (x^2 + b) \sqrt{c - x^2}. \tag{4.5}$$

By rotational invariance the eigenvalues of the other two matrices D_1 and D_2 must be similarly distributed. This means in particular that the model as a whole behaves in the “matrix phase” as a system of 3 decoupled 1-matrix models given by the effective potentials (i fixed)

$$V_{\text{eff}}^{\text{matr}} = \left(\frac{2N}{c} - \frac{3c}{a_{\text{eff}}^2}\right) \text{Tr} D_i^2 + \frac{2}{a_{\text{eff}}^2} \text{Tr} D_i^4, \quad a_{\text{eff}}^2 \equiv \frac{c^2}{2N} + \frac{2cb}{N} = \frac{4c_2 N}{m^2 \tilde{\alpha}_{\text{eff}}^4}. \tag{4.6}$$

N	b	c
24	1047.23 ± 15.97	633.655 ± 0.7516
32	2392.16 ± 65.09	1074.07 ± 1.8680
48	10350.9 ± 236.70	2185.85 ± 1.7130

Table 3. The numerical values of the parameters b and c for different values of N .

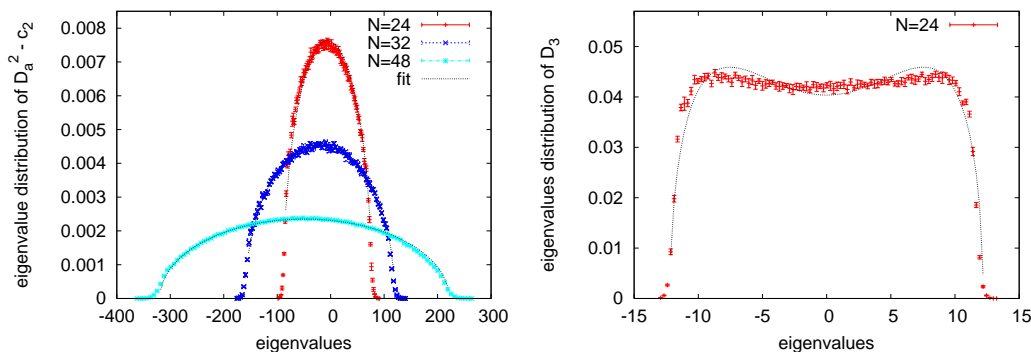


Figure 18. The eigenvalue distributions for D_a^2 , D_3 and $-i[D_1, D_2]$ in the matrix phase for $\tilde{\alpha} = 0.60$ and $m^2 = 200$.

We find numerically table 3. Again the theoretical prediction for a^2 goes like N^3 whereas the effective parameter a_{eff}^2 is found to behave as

$$a_{\text{eff}}^2 = (0.6147 \pm 0.3059) \times N^{3.6580 \pm 0.1553}. \quad (4.7)$$

By going through the same argument which lead to equation (4.4) we can show that $V_{\text{eff}}^{\text{matr}}$ is equivalent to the addition of an extra linear correction in Φ (which depends on c and b or equivalently c and a_{eff}^2) to the classical potential

$$-\frac{4c_2}{a^2} \text{Tr} D_i^2 + \frac{2}{a^2} \text{Tr} D_i^4. \quad (4.8)$$

The result (4.6) accounts for the value $C_v = 0.75$ of the specific heat. Indeed for effective potentials of the form (4.6) each matrix D_i contributes the amount 0.25 .

A final remark is to note that the eigenvalue distributions for $D_a^2 - c_2$ in figure 16 and D_3 in figure 19 clearly depend on N . It would be desirable to find the proper scaling of the parameters for which the distributions are N -independent. This is also related with the predictions of the effective parameters and the corresponding effective potentials written in (4.2) and (4.6).

4.6 Emergent geometry

The sequence of eigenvalue distributions for $\tilde{\alpha} = 0.2, 0.6, 1, 1.5, 2$ and 4 for $m^2 = 200$ and $N = 24$ (figure 20) show clearly that a geometrical phase is emerging as the coupling is increased or equivalently as the temperature is reduced. The geometry that emerges here is that of the fuzzy sphere. This geometry becomes the classical sphere as N is sent to infinity. This is the geometry of the sphere emerging from a pure matrix model and is in our opinion

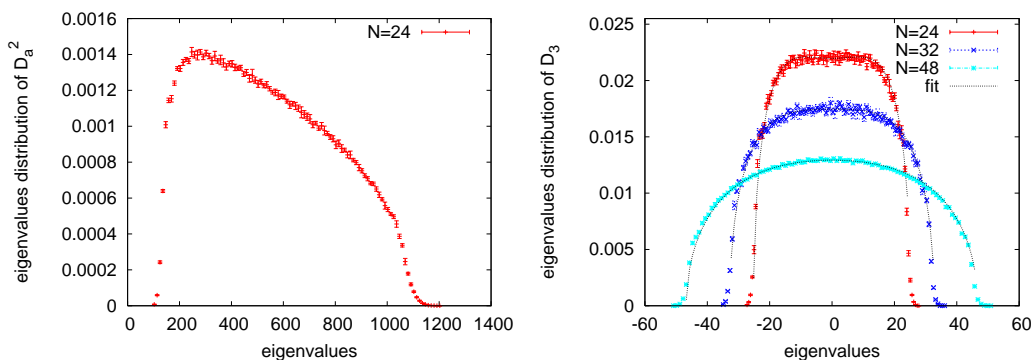


Figure 19. The eigenvalue distributions for D_a^2 for $N = 24$ and D_3 and $-i[D_1, D_2]$ for $N = 24, 32, 48$ in the matrix phase with $\tilde{\alpha} = 0.2$ and $m^2 = 200$. The dashed line corresponds with the fit (4.5) which is the the eigenvalue distribution in the regime of one-cut solution.

a very simple demonstration of a novel concept and opens up the possibility of discussing emergent geometry in a dynamical and statistical mechanical setting. We see clearly that as $\tilde{\alpha}$ is increased from a value deep in the matrix phase to a value well into the fuzzy sphere phase that D_3 goes, from a random matrix with a continuous eigenvalue distribution centered around 0, to a matrix whose eigenvalues are sharply concentrated on the eigenvalues of the rotation generator L_3 . This is also true for the matrices D_1 and D_2 which go over to L_1 and L_2 respectively in the fuzzy sphere phase. This can be seen explicitly in figure 17 since the commutator $[D_1, D_2]$ is found to be well approximated by the matrix iL_3 .

4.7 The model with only pure potential term

The model is given by the potential

$$V[D] = \frac{\tilde{\alpha}^4 m^2}{N} \text{Tr} \left\{ -D_a^2 + \frac{1}{2c_2} (D_a^2)^2 \right\} \quad (4.9)$$

The configurations which minimize this potential are matrices which satisfy $D_a^2 = c_2$. We plot (figure 21) the eigenvalue distributions of the matrices D_3 and D_a^2 for $N = 24$, $m^2 = 200$ and $\tilde{\alpha} = 0.4, 0.6, 1.4$. The distributions of D_a^2 seem to behave in the same way as the distributions of D_a^2 computed in the full model for all values of $\tilde{\alpha}$. The distributions of D_3 are similar to the corresponding distributions of D_3 computed in the full model only in the region of the matrix phase where they are found to fit to the one-cut solution (4.5). In the region of the fuzzy sphere phase the distributions of D_3 tend to split into two cuts. However they never achieve this splitting completely due to the mixing terms $\text{Tr} D_1^2 D_2^2$, $\text{Tr} D_1^2 D_3^2$ and $\text{Tr} D_2^2 D_3^2$. These terms cannot be neglected for values of the coupling $\tilde{\alpha}$ where the model is in the fuzzy sphere phase.

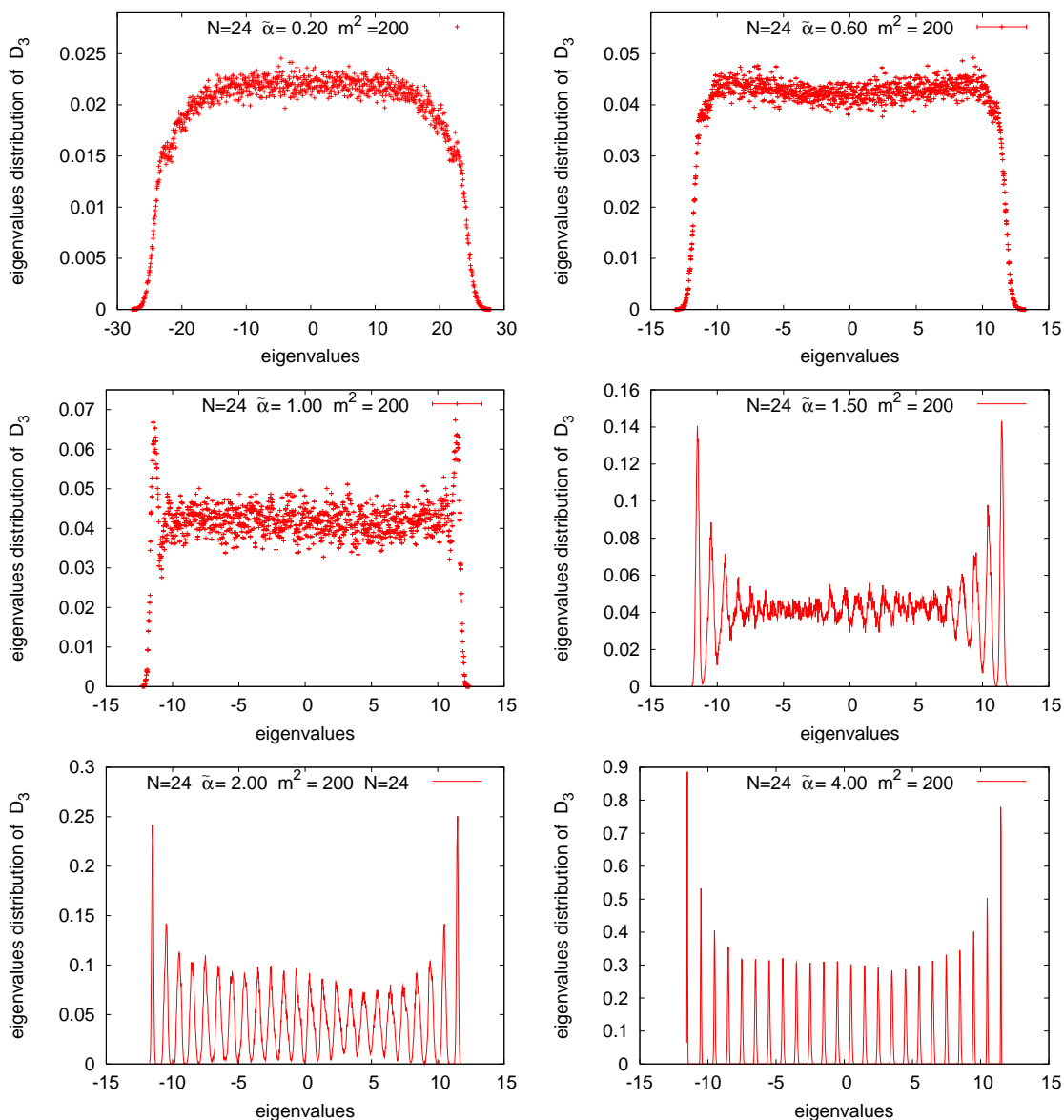


Figure 20. The model undergoes a transition from the matrix phase with no underlying geometry to a geometrical phase as the coupling constant $\tilde{\alpha}^4 = \frac{1}{T}$ is increased (or the temperature lowered). The geometry which emerges in this model is the geometry of the sphere.

4.8 The Chern-Simons+potential model

In this final section we present the eigenvalue distributions for the model in which we set the Yang-Mills term to zero. The action reduces to

$$S[D] = \frac{1}{g^2 N} \text{Tr} \left[\frac{i}{3} \epsilon_{abc} [D_a, D_b] D_c + \frac{m^2}{2c_2} (D_a^2 - c_2)^2 \right]. \quad (4.10)$$

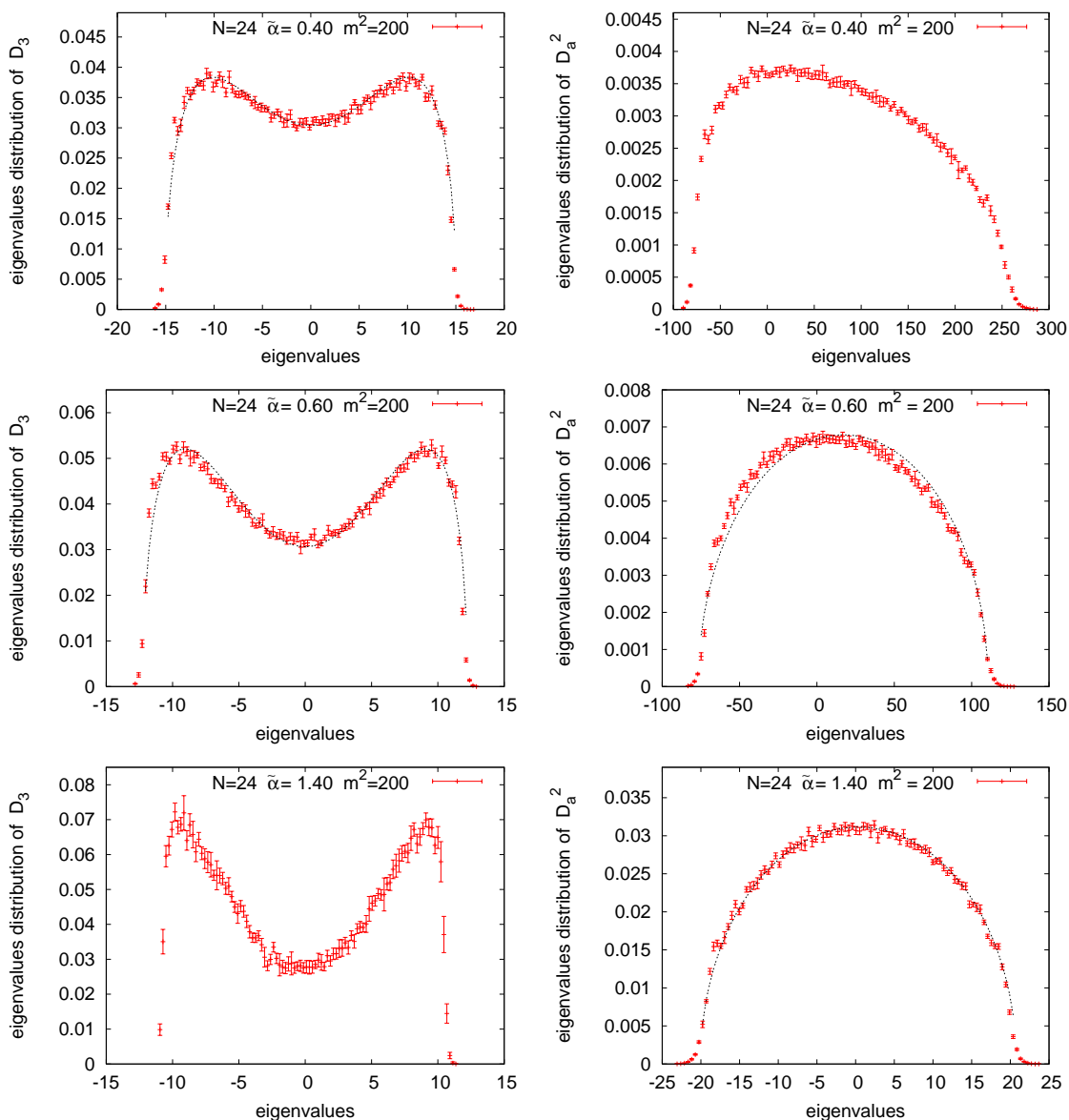


Figure 21. The eigenvalue distributions of D_a^2 and D_3 for the pure potential term. Deep inside the nonperturbative regime (small $\tilde{\alpha}$ or large temperature) the distribution for D_3 is in the one-cut solution (4.5) whereas for large $\tilde{\alpha}$ (or low temperature) the eigenvalue distribution for D_a^2 is given by the Wigner semi-circle law.

The equations of motion are

$$i\epsilon_{abc}[D_b, D_c] - 2m^2 D_a + \frac{m^2}{c_2} \{D_c^2, D_a\} = 0. \tag{4.11}$$

The possible solutions are the commuting matrices and reducible representations of $SU(2)$.

We measure the eigenvalue distributions of the matrix D_3 for different values of $\tilde{\alpha}$. The distributions of D_3 in the region of the matrix phase can be fit to the one-cut solution (4.5).

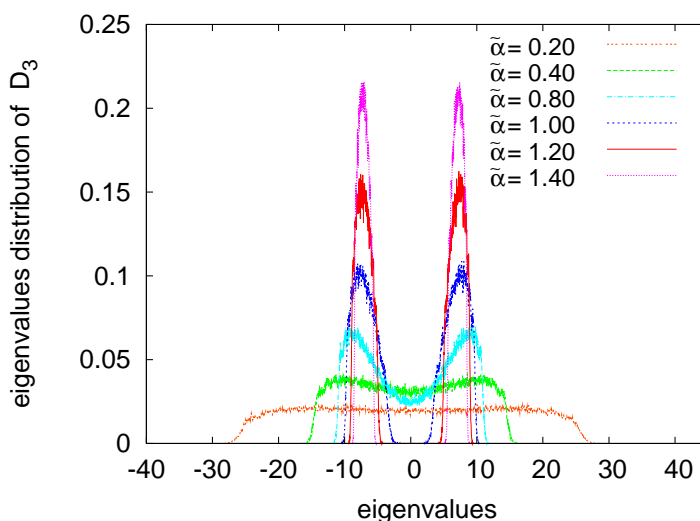


Figure 22. The eigenvalue distributions of D_3 for the Chern-Simons + Potential model for different values of the coupling $\tilde{\alpha}$ for $N = 24$ and $m^2 = 200$. In this case, the system undergoes a transition from the one-cut regime to the two-cut regime as the coupling (or temperature) is increased (lowered).

In the region of the fuzzy sphere phase the distributions of D_3 split into two well separated cuts. See figure 22. This model exhibits therefore the behaviour of a typical quartic one-matrix model. The value of the coupling $\tilde{\alpha}$ where the transition from the one-cut phase to the two-cut phase happens coincides with the maximum of the specific heat. From the numerical results we can also see that in the regime of large $\tilde{\alpha}$ the preferred configurations are given by

$$D_a = 2\lambda \frac{\sigma_a}{2} \otimes \mathbf{1}_{\frac{N}{2}}. \tag{4.12}$$

λ is fixed by the requirement $D_a^2 = c_2$, i.e $3\lambda^2 = c_2$ and σ_a are the Pauli matrices. Indeed the eigenvalue distributions of the matrices D_a^2 , $D_a D_b D_a D_b$, $D_a D_b D_b D_a$ and $i\epsilon_{abc} D_a D_b D_c$ for large $\tilde{\alpha}$ are found (figure 23) to be given by the Wigner semi circle laws

$$\rho(x) = \frac{2}{a^2\pi} \sqrt{a^2 - (x - x_0)^2}. \tag{4.13}$$

The centers x_0 are given by the theoretical values

$$\begin{aligned} D_a^2 &= 3\lambda^2 \mathbf{1}_N \\ D_a D_b D_a D_b &= -3\lambda^4 \mathbf{1}_N \\ D_a D_b D_b D_a &= 9\lambda^4 \mathbf{1}_N \\ i\epsilon_{abc} D_a D_b D_c &= -6\lambda^3 \mathbf{1}_N. \end{aligned} \tag{4.14}$$

For instance in figure 23 we can see from the eigenvalue distribution of D_3 with $N = 24$, $\tilde{\alpha} = 4$ and $m^2 = 200$ that the preferred configurations are given by (4.12) with $\lambda = \pm(7.16 \pm 0.25)$ whereas the predicted value is $\lambda = \pm 6.9567$. We also remark that the eigenvalue distributions of D_a^2 and the other operators have the same structure as in the full model in its matrix phase.

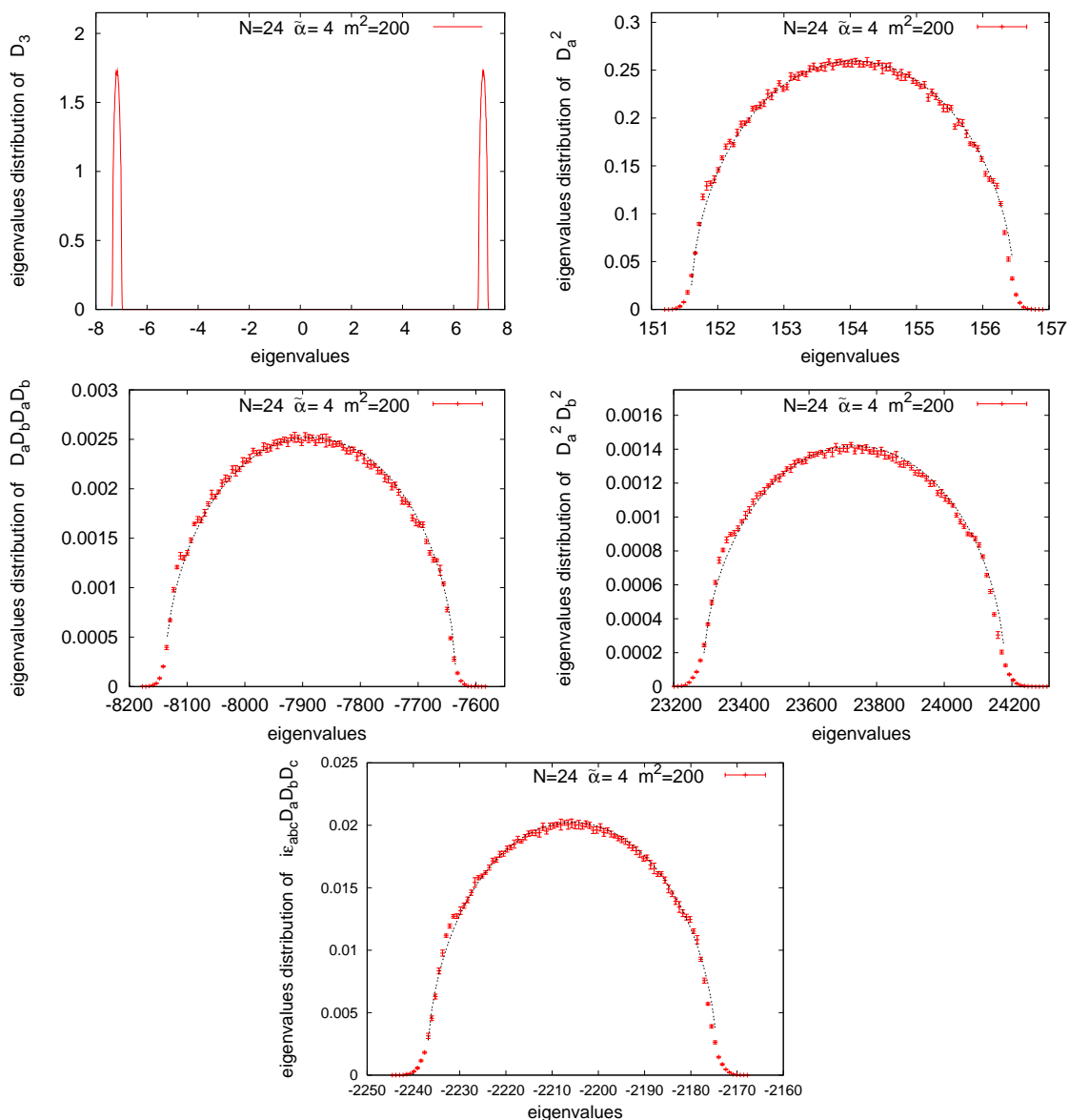


Figure 23. The eigenvalue distributions of D_3 , D_a^2 , $D_a D_b D_a D_b$, $D_a D_b D_b D_a$, $i\epsilon_{abc} D_a D_b D_c$ for the Chern-Simons+potential model. The solid lines correspond to the Wigner semicircle laws with centers given by eqs. (4.14).

5 Conclusion and outlook

We have studied the simple three matrix model with Euclidean action functional (3.6) for general values of its parameters $\beta = \tilde{\alpha}^4$ and m but focused on a small range of the possible values of the parameter μ .

We find the model to have two clearly distinct phases. In the high temperature regime (i.e. small $\tilde{\alpha}$) the model has a disordered phase. In this phase the eigenvalues distribution of an individual matrix is well approximated by the one-cut distribution of a hermitian matrix model with quartic potential. We call this phase the *matrix phase* of the model.

At low temperature the model has an ordered phase. The order is unusual in that it describes the condensation of a background geometry as a collective order of the matrix degrees of freedom. We call this the *geometrical* or *fuzzy sphere phase*, since for finite matrix size the ground state is described by a fuzzy sphere which is a quantized version of the classical sphere. In the large matrix size limit the sphere becomes classical but at a microscopic level the geometry always has a noncommutative character as can be seen from the spectrum of the “coordinate functions” which are proportional to the $su(2)$ generator L_3 in the irreducible representation of dimension given by the matrix size.

In the geometrical phase small fluctuations are those of a $U(1)$ gauge field and a neutral scalar field fluctuating on a round two sphere. The two fields have non-trivial mixing at the quadratic level but are otherwise not interacting. In this phase, with $\mu = m^2$, the parameter m^2 parameterizes the mass of the scalar fluctuation, otherwise for $\mu = m^2 - \rho/N$, the parameter ρ provides a constant external current for the scalar field.

For $m = \mu = 0$ the transition between the two phases is found to be discontinuous. There is a jump in the internal energy (expectation of the Euclidean action) and from a theoretical analysis (valid in the fuzzy sphere phase) we find the entropy drops by $1/9$ per degree of freedom [15] as one crosses from the high temperature matrix phase to the geometrical one. Our theoretical results also predict that: For all m and $\mu > -\frac{2}{9}$, the model has divergent critical fluctuations in the specific heat characterised by the critical exponent $\alpha = 1/2$. The critical regime narrows as the critical temperature decreases and the transition temperature is sent to zero at $\mu = -\frac{1}{4}$ and so there is no geometrical phase beyond this point.

Our numerical simulations are in excellent agreement with these theoretical predictions and we find the critical fluctuations are only present in the fuzzy sphere phase so that the transition has an asymmetrical character. We know of no other physical setting that exhibits transitions of the type presented here and further numerical and theoretical study are needed. However, the thermodynamic properties of the transition are similar to those found in the 6-vertex model and the dimer model [33, 34].

We focus simulations on $\mu = m^2$ and observe that the discontinuity in the entropy (or the latent heat) decreases as m^2 is increased with the jump vanishing for sufficiently large m . We have not been able to determine with precision where the transition becomes continuous, however the jump in the entropy becomes too small to measure beyond $m^2 \sim 40$. Also, the predicted critical fluctuations are not seen in the numerical results for large m^2 .

The data for the critical point coupling, from our different methods of estimating it, separate in the parameter range where the latent heat disappears indicating a possible multi-critical point or richer structure. For larger values of $m^2 = \mu$ we have not been able to resolve the nature of the transition. The numerical evidence shows the structure of a 3rd order transition, a behaviour typical of many matrix models, however, the fact that $\tilde{\alpha}_s$, the crossing point of the average action curves for different N , still reliably predicts the transition line, suggests the transition is continuous with asymmetric critical fluctuations, consistent with the theoretical analysis.

Our conclusion is that the full model has the qualitative features of the model with $m = \mu = 0$ (model S_0 of eq. (3.3)) and that the effect of the potential is to shift the

transition temperature and provide a non-trivial background specific heat. The divergence of the specific heat arises from the interplay of the Chern-Simons and Yang-Mills terms. Given that this competition leads to a divergent specific heat, we expect, sufficiently close to the transition, to see the effect of this competition emerge and the specific heat to eventually rise above the background provided by the potential and diverge as the critical point.

The model of emergent geometry described here, though reminiscent of the random matrix approach to two dimensional gravity [4] is in fact very different. The manner in which spacetime emerges is also different from that envisaged in string pictures where continuous eigenvalue distributions [3] or a Liouville mode [23] give rise to extra dimensions. It is closely connected to the $D0$ brane scenario described in [12] and the $m = 0$ version is a dimensionally reduced version of a boundary WZNW models in the large k limit [13]. A two matrix model where the large N limit describes a hemispherical geometry was studied in [32]. It is not difficult to invent higher dimensional models with essentially similar phenomenology to that presented here (see [19, 21] and [20]). For example any complex projective space \mathbf{CP}^N can emerge from pure matrix dynamics by choosing similar matrix models with appropriate potentials [19].

In summary, we have found an exotic transition in a simple three matrix model. The nature of the transition is very different if approached from high or low temperatures. The high temperature phase is described by three decoupled random matrices with self interaction so there is no background spacetime geometry. As the system cools a geometrical phase condenses and at sufficiently low temperatures the system is described by small fluctuations of a $U(1)$ gauge field coupled to a massive scalar field. The critical temperature is pushed upwards as the scalar field mass is increased. Once the geometrical phase is well established the specific heat takes the value 1 with the gauge and scalar fields each contributing $1/2$.

We believe that this scenario gives an appealing picture of how a geometrical phase might emerge as the system cools and suggests a very novel scenario for the emergence of geometry in the early universe. In such a scenario the temperature can be viewed as an effect of other degrees of freedom present in a more realistic model but not directly participating in the transition we describe. In the model described in detail above, both the geometry and the fields are emergent dynamical concepts as the system cools. Once the geometry is well established the background scalar decouples from the rest of the physics and is always massive. If a realistic cosmological model can be found, such decoupled matter should provide a natural candidate for dark matter.

Acknowledgments

The work of B.Y is supported by a Marie Curie Fellowship from The Commission of the European Communities under contract number MIF1-CT-2006-021797. The work of R.D.B. is supported by CONACYT México. R.D.B would also like to thank the Institute für Physik, Humboldt-Universität zu Berlin for their hospitality and support while this work was in progress. In particular he would like to thank Prof. Michael Müller-Preussker and Mrs. Sylvia Richter.

References

- [1] A. Connes, *Noncommutative geometry*, Academic Press, London U.K. (1994).
- [2] L. Bombelli, J.-H. Lee, D. Meyer and R. Sorkin, *Space-time as a causal set*, *Phys. Rev. Lett.* **59** (1987) 521 [[SPIRES](#)].
- [3] N. Seiberg, *Emergent spacetime*, [hep-th/0601234](#) [[SPIRES](#)].
- [4] J. Ambjørn, R. Janik, W. Westra and S. Zohren, *The emergence of background geometry from quantum fluctuations*, *Phys. Lett.* **B 641** (2006) 94 [[gr-qc/0607013](#)] [[SPIRES](#)].
- [5] T. Azuma, S. Bal, K. Nagao and J. Nishimura, *Nonperturbative studies of fuzzy spheres in a matrix model with the Chern-Simons term*, *JHEP* **05** (2004) 005 [[hep-th/0401038](#)] [[SPIRES](#)].
- [6] P. Castro-Villarreal, R. Delgadillo-Blando and B. Ydri, *A gauge-invariant UV-IR mixing and the corresponding phase transition for U(1) fields on the fuzzy sphere*, *Nucl. Phys.* **B 704** (2005) 111 [[hep-th/0405201](#)] [[SPIRES](#)].
- [7] D. O'Connor and B. Ydri, *Monte Carlo simulation of a NC gauge theory on the fuzzy sphere*, *JHEP* **11** (2006) 016 [[hep-lat/0606013](#)] [[SPIRES](#)].
- [8] B. Ydri, *Fuzzy physics*, [hep-th/0110006](#) [[SPIRES](#)].
- [9] D. O'Connor, *Field theory on low dimensional fuzzy spaces*, *Mod. Phys. Lett.* **A 18** (2003) 2423 [[SPIRES](#)].
- [10] A.P. Balachandran, S. Kurkcuglu and S. Vaidya, *Lectures on fuzzy and fuzzy SUSY physics*, [hep-th/0511114](#) [[SPIRES](#)].
- [11] H. Grosse, C. Klimčik and P. Prešnajder, *Finite quantum field theory in noncommutative geometry*, *Commun. Math. Phys.* **180** (1996) 429 [[hep-th/9602115](#)] [[SPIRES](#)].
- [12] R.C. Myers, *Dielectric-branes*, *JHEP* **12** (1999) 022 [[hep-th/9910053](#)] [[SPIRES](#)].
- [13] A.Y. Alekseev, A. Recknagel and V. Schomerus, *Brane dynamics in background fluxes and non-commutative geometry*, *JHEP* **05** (2000) 010 [[hep-th/0003187](#)] [[SPIRES](#)].
- [14] J. Hoppe, *Quantum theory of a massless relativistic surface and a two-dimensional bound state problem*, Ph.D. Thesis, MIT, Cambridge, Massachusetts, U.S.A. (1982);
J. Madore, *The fuzzy sphere*, *Class. Quant. Grav.* **9** (1992) 69 [[SPIRES](#)].
- [15] R. Delgadillo-Blando, D. O'Connor and B. Ydri, *Geometry in transition: a model of emergent geometry*, *Phys. Rev. Lett.* **100** (2008) 201601 [[arXiv:0712.3011](#)] [[SPIRES](#)].
- [16] H. Steinacker, *Quantized gauge theory on the fuzzy sphere as random matrix model*, *Nucl. Phys.* **B 679** (2004) 66 [[hep-th/0307075](#)] [[SPIRES](#)].
- [17] T. Azuma, K. Nagao and J. Nishimura, *Perturbative dynamics of fuzzy spheres at large-N*, *JHEP* **06** (2005) 081 [[hep-th/0410263](#)] [[SPIRES](#)].
- [18] H. Steinacker and R.J. Szabo, *Localization for Yang-Mills Theory on the fuzzy sphere*, *Commun. Math. Phys.* **278** (2008) 193 [[hep-th/0701041](#)] [[SPIRES](#)].
- [19] D. Dou and B. Ydri, *Topology change from quantum instability of gauge theory on fuzzy CP²*, *Nucl. Phys.* **B 771** (2007) 167 [[hep-th/0701160](#)] [[SPIRES](#)].
- [20] N. Kawahara, J. Nishimura and S. Takeuchi, *Exact fuzzy sphere thermodynamics in matrix quantum mechanics*, *JHEP* **05** (2007) 091 [[arXiv:0704.3183](#)] [[SPIRES](#)].

- [21] H. Steinacker, *Emergent gravity from noncommutative gauge theory*, *JHEP* **12** (2007) 049 [[arXiv:0708.2426](#)] [[SPIRES](#)].
- [22] P. Di Francesco, P.H. Ginsparg and J. Zinn-Justin, *2-D gravity and random matrices*, *Phys. Rept.* **254** (1995) 1 [[hep-th/9306153](#)] [[SPIRES](#)].
- [23] V.G. Knizhnik, A.M. Polyakov and A.B. Zamolodchikov, *Fractal structure of 2d-quantum gravity*, *Mod. Phys. Lett. A* **3** (1988) 819 [[SPIRES](#)].
- [24] S. Minwalla, M. Van Raamsdonk and N. Seiberg, *Noncommutative perturbative dynamics*, *JHEP* **02** (2000) 020 [[hep-th/9912072](#)] [[SPIRES](#)].
- [25] J. Fröhlich and K. Gawędzki, *Conformal field theory and geometry of strings*, Lectures given at *Mathematical quantum theory conference*, Vancouver, Canada, 4-8 Aug 1993, published in Vancouver 1993, in *Proceedings of Mathematical quantum theory* **Vol. 1** pg. 57–97 [[hep-th/9310187](#)] [[SPIRES](#)].
- [26] H. Grosse and J. Madore, *A noncommutative version of the Schwinger model*, *Phys. Lett. B* **283** (1992) 218 [[SPIRES](#)].
- [27] U. Carow-Watamura and S. Watamura, *Differential calculus on fuzzy sphere and scalar field*, *Int. J. Mod. Phys. A* **13** (1998) 3235 [[q-alg/9710034](#)] [[SPIRES](#)].
- [28] U. Carow-Watamura and S. Watamura, *Noncommutative geometry and gauge theory on fuzzy sphere*, *Commun. Math. Phys.* **212** (2000) 395 [[hep-th/9801195](#)] [[SPIRES](#)].
- [29] H. Grosse, J. Madore and H. Steinacker, *Field theory on the q-deformed fuzzy sphere. I*, *J. Geom. Phys.* **38** (2001) 308 [[hep-th/0005273](#)] [[SPIRES](#)].
- [30] T. Azuma, S. Bal and J. Nishimura, *Dynamical generation of gauge groups in the massive Yang-Mills-Chern-Simons matrix model*, *Phys. Rev. D* **72** (2005) 066005 [[hep-th/0504217](#)] [[SPIRES](#)].
- [31] L.D. Faddeev and V.N. Popov, *Feynman diagrams for the Yang-Mills field*, *Phys. Lett. B* **25** (1967) 29 [[SPIRES](#)].
- [32] D.E. Berenstein, M. Hanada and S.A. Hartnoll, *Multi-matrix models and emergent geometry*, *JHEP* **02** (2009) 010 [[arXiv:0805.4658](#)] [[SPIRES](#)].
- [33] C. Nash and D. O'Connor, *Topological phase transitions and holonomies in the Dimer model*, *J. Phys. A* **42** (2009) 012002 [[arXiv:0809.2960](#)] [[SPIRES](#)].
- [34] E.H. Lieb, *Exact solution of the two-dimensional Slater KDP model of a ferroelectric*, *Phys. Rev. Lett.* **19** (1967) 108 [[SPIRES](#)].